

Application of Endurance Time Method in Seismic Assessment of RC Frames Designed by Direct Displacement-Based Procedure

Nisar Ahmad KARIMZADA¹
Amir SHIRKHANI²
Engin AKTAŞ^{3*}



ABSTRACT

This paper addresses the Direct Displacement-Based Design (DDBD) approach of multi-story RC frame structures consistent with changes to design criteria between Turkish earthquake codes of TSC-2007 and TBEC-2018. The corresponding response modification factor (R) of structures designed based on the DDBD approach is also estimated in this research. The design base shear forces of both codes are compared considering different R factors and also with that of the DDBD approach. The results showed that the DDBD approach, as per TBEC-2018, provides RC frame structures with higher R values compared to the similar approach in accordance with TSC-2007. The Endurance Time (ET) method is a time history-based procedure for seismic assessment of structures under intensifying dynamic excitations aided to judge their performance at various intensity levels. Since, up to now, the ET method has not been considered to evaluate the performance of the structures designed by the DDBD approach, this paper addresses this issue. The ET performance curves of RC frames show that structures designed by the DDBD approach in accordance with TBEC-2018 exhibit higher Interstory Drift Ratios (IDRs) values than TSC-2007 at various hazard levels.

Keywords: Direct displacement-based design, endurance time method, endurance time excitation function, interstory drift ratio, performance curve, pushover analysis, response modification factor.

Note:

- This paper was received on January 20, 2023 and accepted for publication by the Editorial Board on October 13, 2023.
- Discussions on this paper will be accepted by May 31, 2024.
- <https://doi.org/10.18400/tjce.1239730>

1 İzmir Institute of Technology, Department of Civil Engineering, İzmir, Türkiye
nissarahmadkarimzada3@gmail.com - <https://orcid.org/0000-0002-0915-5397>

2 University of Tabriz, Department of Structural Engineering, Tabriz, Iran
shirkhani@tabrizu.ac.ir - <https://orcid.org/0000-0003-2532-2906>

3 İzmir Institute of Technology, Department of Civil Engineering, İzmir, Türkiye
enginaktas@iyte.edu.tr - <https://orcid.org/0000-0002-5706-2101>

* Corresponding author

1. INTRODUCTION

Structures should be designed in such a way that they can resist different types of static and dynamic loads applied to them. The design of structures to such loads is guided through standards and codes. One of the dynamic loads is due to earthquakes, which poses a challenge for a structural engineer to design a structure to perform safely against. Traditional Seismic Design Codes (TSDCs) used for such purposes have been developed for several years based on Force-Based Design (FBD) and some linear elastic concepts. Furthermore, the Life Safety (LS) performance level under the design earthquake (10% probability of exceedance in 50 years) has been considered in such codes. Most of the TSDCs do not address the inelastic response of the structures directly in the design stage and thus cannot effectively deal with the damage due to structural, nonstructural, and content systems [1]. However, there are some modern codes that consider the inelastic response of the structures directly in the design stage. In addition, no clear information regarding economic losses and downtime is provided in the TSDCs [2]. The Performance-Based Seismic Design (PBSD) approach is a fairly new paradigm for the seismic assessment and retrofitting of existing structures and seismic design of new structures, which has attracted the attention of researchers for around the last two decades. It is a considerably reliable approach, and it promises to produce structures with a more realistic understanding of the risk of casualties, occupancy interruption, and economic losses which could occur as a result of future earthquakes [2]. The structure designed using the PBSD approach is expected to achieve the specific performance objectives selected prior to design, given certain hazard levels. Furthermore, it deals with the outcome of the structure rather than prescribing how it is to be built, and the ultimate goal is used as a starting point for the design purpose. In addition, it is capable of reducing the life cycle cost of the structure under a specific earthquake hazard level. It is also able to give more detailed information about the performance of structural, nonstructural, and content systems.

Different methods could be used in the PBSD framework, such as the N2 method, capacity spectrum method, Direct Displacement-Based Design (DDBD) method, etc. A performance objective is the combination of a performance level and a hazard level. Performance level can be determined by damage states of structural and nonstructural and content systems [3]. In this study, the DDBD approach is adopted since displacement has a direct relation with damage states of the structural and nonstructural components [4]. The Displacement-Based Design (DBD) procedure appeared in the 1990s for the design of structures, which drew the attention of the researchers. As a consequence, different DBD methodologies were developed. Major research devoted to this methodology are Chopra and Goel [5], Moehle [6], Panagiotakos and Fardis [7], Priestley and Kowalsky [8] for RC structures, and Medhekar and Kennedy [9, 10] for steel structures. Among the DBD methodologies, the most widely used one is the DDBD approach, first introduced by Priestley [11]. A critical review was provided by Sullivan et al. [12] into different DBD approaches, and a comparison between the DDBD approach and other DBD methodologies has been reported. A textbook by Priestley et al. [13] covers comprehensively the DDBD approach for seismic design of RC, steel, and timber buildings as well as buildings with isolation and supplemental damping devices. Besides, a model code DBD12 by Sullivan et al. [14] has also gained wide acceptance.

Remarkable studies have been conducted to develop the DDBD approach for different structural systems, such as RC structures, steel structures, masonry and timber structures,

bridges, and structures equipped with seismic isolation systems. Pettinga and Priestley [15] investigated the dynamic behavior of reinforced concrete tube frames designed with the DDBD approach. They proposed some modifications considering the higher mode's effects, specifically for buildings taller than 10 stories. Sullivan et al. [16] developed the DDBD procedure for RC dual-wall frame structures. The applicability of the DDBD approach for near-fault areas was investigated by Moghim and Saadatpour [17]. The suitability of the DDBD approach for the seismic design of precast concrete structures is conducted by Belleri [18] regarding the effect of the foundation flexibility, beam-to-column, and foundation-to-column connections. Sullivan and Lago [19] proposed a new methodology for DDBD of moment-resisting frames with viscous dampers. Malekpour and Dashti [20] investigated the DDBD approach for different RC structural systems, including moment-resisting, dual wall-frame and dual steel-braced systems.

Furthermore, using the elastoplastic single degree of freedom (SDOF) systems, the P-delta effect is investigated extensively for both DDBD and FBD approaches by Pourali et al. [21]. Seismic performance evaluation of low and medium-rise concentrically braced frames, designed using the DDBD approach, is carried out by Sahoo and Prakash [22]. Yan and Gong [23] developed a displacement profile expression for the DDBD method of regular RC frame structures. Giannakouras and Zeris [24] used the DDBD approach for the seismic design of RC frames with setback irregularity accounting for local ductility associated with global behavior. Kumbhar et al. [25] used six distinct DDBD approaches developed by various researchers for the design of low-, medium-, and high-rise RC frame buildings and compared their seismic performance. Malla and Wijeyewickrema [26] developed the DDBD approach for the coupled walls with steel shear link coupling beams using inelastic displacement spectra. Papagiannopoulos et al. [27] presented numerical examples of the eccentrically and concentrically braced steel frames to explain the DDBD approach and its advantages. Sharma et al. [28] investigated the inelastic behavior of low and mid-rise RC buildings designed by FBD and DDBD. Mohebbi et al. [29] extended the DDBD approach for the isolated structures equipped with viscous dampers and assessed the seismic performance of the structures for near and far-field earthquakes. Kalapodis et al. [30] improved the DDBD approach for three types of plane steel frames, namely moment-resisting frames, steel concentrically braced frames, and buckling-restrained braced frames.

The Endurance Time (ET) method initially introduced by Estekanchi et al. [31] is a rather fast incremental-based dynamic time history analysis in which structures experience intensifying dynamic excitations. The response of the structure is predicted by this method considering the relationship between Intensity Measures (IMs) and Engineering Demand Parameters (EDPs)[32]. The EDPs characterize the structural response, whereas IMs characterize the ground shaking intensity at different seismic hazard levels. In this method, structural response for a continuous range of IMs is provided by a single Nonlinear Time History Analysis (NTHA); however, traditional NTHA provides the structural response at a single IM level. In fact, the ET method represents the structural response at various IM levels using the least number (commonly three) of NTHA [32], which is conventionally provided by Incremental Dynamic Analysis (IDA). Several studies have been conducted on the ET method in recent years [33–39], and the validity of ET results has been confirmed by comparing them with the results of NTHA [40–45]. These research works compared the results of NTHA under 7 or 22 Ground Motion (GM) records with the ET method results under three simulated Endurance Time Excitation Functions (ETEFs) records. They showed

that the results of the ET method were sufficiently close to the results of the NTHA under GM records.

The Turkish Building Earthquake Code 2018 (TBEC-2018) replaced the previous code, the Turkish Seismic Code 2007 (TSC-2007), in 2019. Compared to TSC-2007 [46], significant changes have been made in TBEC-2018 [47], similar to ASCE 7-16 and comprising new design approaches. In this paper, an adaptive approach for the DDBD is presented with respect to the changes to Turkish seismic design criteria, for RC frame buildings. To this end, multi-story RC frame structures are considered here and designed based on the DDBD approach in compliance with both mentioned seismic design codes. For the detailed design purpose, i.e., flexural and shear design of columns and beams, TS500 Turkish Standards [48] is used together with the procedure given by Ersoy et al. [49]. Capacity design principles are applied to obtain a structure with the desired beam sway mechanism, i.e., a structure with strong-column weak-beam, in which plastic hinges form in beams rather than in columns.

This research generally pursues the following objectives: (i) First, designing multi-story RC frame structures using the DDBD approach in accordance with TSC-2007 and TBEC-2018 and comparing their results. (ii) Second, obtaining base shear forces for the selected RC frames using TSC-2007 and TBEC-2018 through the Equivalent Lateral Force (ELF) method for different response modification factors. A comparison between the base shear forces obtained based on TSC-2007 and TBEC-2018 is also made. These base shear forces are also compared to those obtained through the DDBD approach. (iii) Third, since estimating the response modification factors of the structures based on the DDBD approach has been less considered in the previous studies, this issue is also addressed in this paper. Hence, the actual response modification factors for each frame designed using the DDBD approach in accordance with TSC-2007 and TBEC-2018 are estimated, and their results are compared. To this end, nonlinear static pushover analyses are performed on the structures. (iv) Since up to now the ET method has not been used to assess the behavior of the structures designed by the DDBD approach, it is also considered here. To consider the impact of ground motion duration on the structural responses, the fourth generation of ETEFs [32, 40] is used in this study, which is including the cumulative absolute velocity (CAV) in its generation process.

2. SEISMIC DESIGN CODES USED IN THIS STUDY

Türkiye is located in a seismically active region. The North Anatolian Fault (NAF) and the East Anatolian Fault are two active faults that are responsible for many major earthquakes in Türkiye. The earthquake design code for buildings was published for the first time in Türkiye in 1940 after the Erzincan earthquake occurred in 1939, with a magnitude of 7.9 [50]. The earthquake code was then revised and improved several times due to the design deficiencies observed during the construction phase and also concerning technological and social development in society [51].

2.1. Difference of Criteria of Seismic Design Codes Used in This Study

After the Gölcük earthquake in 1999 with a magnitude of 7.4, TSC-2007 was published in 2007. A new chapter is included in TSC-2007 for the assessment and rehabilitation of the existing buildings. Furthermore, linear and nonlinear methods are considered in this

regulation. The last version of the earthquake code for buildings in Türkiye was published in March 2018, “Turkish Building Earthquake Code (TBEC-2018)”. This version has many changes with respect to TSC-2007, most of which are similar to ASCE 7-16 [51, 52]. Some of these changes are made in site classes, importance factors, occupancy category, period calculation, overstrength factor, response modification factor, or behavior factor [52].

One of the most important differences between these codes is the calculation of the elastic acceleration response spectrum used in this study. One of the required parameters for calculating the elastic response spectrum in TSC-2007 is the effective ground acceleration coefficient (A_0), which depends on the seismic zone. Seismic zones are divided into 4 different zones in TSC-2007, Zone 1 with the highest seismicity and Zone 4 with the lowest seismicity. However, in TBEC-2018, seismic hazard maps are used instead of seismic zones, from which mapped values of Maximum Considered Earthquake (MCE_R) spectral response acceleration parameters at one second (S_1) and at the short period (S_S) are obtained. Moreover, spectrum characteristic periods (T_A and T_B) are the other parameters required for calculating the elastic acceleration response spectrum, which depends on the local site class in TSC-2007. In contrast, these values are obtained using the provided equations in TBEC-2018, which depends on S_1 and S_S . For more detailed information about obtaining the elastic acceleration response spectrum, the reader is referred to TSC-2007 and TBEC-2018.

3. DIRECT DISPLACEMENT-BASED SEISMIC DESIGN APPROACH

Priestley and Kowalsky [8] proposed the DDBD approach for the design of RC structures. It is based on the PBSD method, and it is a simple design procedure widely accepted by researchers [20]. While FBD utilizes the acceleration response spectrum to calculate the global base shear for the structure, the DDBD approach utilizes the displacement response spectrum to estimate the global base shear; further, the maximum inelastic deformation of the structure is considered. Figure 1 is adopted from Priestley and Kowalsky [8], which provides the fundamentals of the DDBD approach. From Figure 1, it is evident that a Multi Degree of Freedom (MDOF) system is presented by an equivalent Single Degree of Freedom (SDOF) system. The equivalent SDOF system involves effective height (H_e) and effective mass (m_e), Figure 1(a). The maximum displacement of the SDOF system is presented with effective stiffness (K_{eff}), Figure 1(b), and equivalent viscous damping (ξ_{eq}), Figure 1(c). As can be seen that the effective stiffness of SDOF systems is significantly lower than the initial stiffness of the structure, which in turn gives lower base shear force [8]. The reason is that the SDOF system presents the MDOF system at the maximum inelastic response [53].

The first step in the procedure of the DDBD approach is to choose a performance level that corresponds to a specific ground motion hazard. Since damage is directly related to displacement, the IDR is selected. Then, using this ratio, target design displacement, and ductility demand are obtained. The ductility demand is used to obtain the equivalent viscous damping (ξ_{eq}); refer to Figure 1(c). The equivalent viscous damping is used to reduce the elastic design displacement response spectrum (elastic design displacement response spectrum is obtained for a 5% damping ratio). Finally, the effective period is obtained from

the reduced design displacement response spectrum, which can be used then to obtain the effective stiffness and base shear forces, respectively.

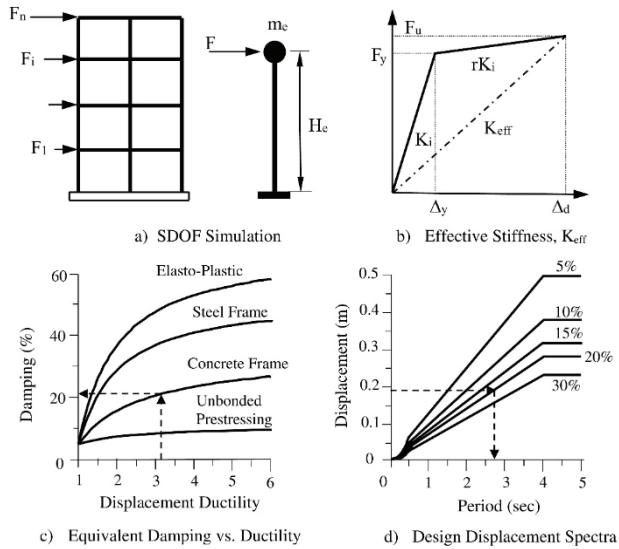


Figure 1 - Fundamentals of the DDBD approach [8].

A simple framework for the DDBD procedure is given in Figure 2. It starts with the selection of target displacement and ends with the determination of base shear force.

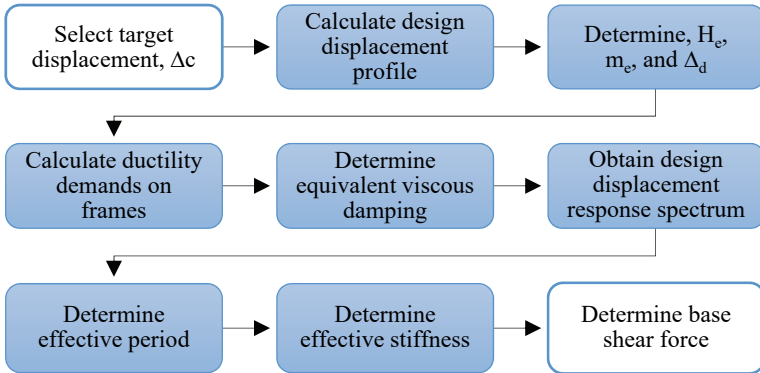


Figure 2 - Framework of the DDBD approach.

After selecting the drift ratio, target displacement (Δ_C) is obtained, and this value is used to obtain the design story displacement (Δ_i). To this end, the normalized inelastic mode shape (δ_i) should be found as follows [8]:

$$\delta_i = \frac{H_i}{H_n} \quad \text{for } n \leq 4 \quad (1)$$

$$\delta_i = \frac{4}{3} \left(\frac{H_i}{H_n} \right) \left(1 - \frac{H_i}{4H_n} \right) \quad \text{for } n > 4 \quad (2)$$

In these equations, H_i is the story height from the ground/foundation level, H_n is the total height of the frame, and n is the number of stories. In addition, these equations have been shown to be sufficient for the design purpose by Pettinga [54]. It has been shown that the design displacement profile obtained using these two equations reasonably matches the displacement profile obtained from the time history analysis [13, 54]. The design displacement at the top of each story, Δ_i can be calculated as follows:

$$\Delta_i = \omega_\theta \delta_i \frac{\Delta_c}{\delta_c} \quad (3)$$

where δ_c and Δ_c are the inelastic mode shape and design displacement of the critical story (the story with the largest drift ratio), respectively. ω_θ is the drift reduction factor to take into account the higher mode effects. It will have negligible effects for the number of stories less or equal to 10 ($n \leq 10$), and it can be obtained as follows [55]:

$$\omega_\theta = 1.15 - 0.0034H_n \leq 1.0 \quad (4)$$

Target design displacement (Δ_c) is obtained as follows:

$$\Delta_c = \theta_d H_c \quad (5)$$

where H_c and θ_d the height of the critical story from the ground/foundation level and IDR, chosen as performance level for a specific ground motion intensity.

Once the design displacement profile is obtained, then it is used to obtain the design displacement (Δ_d) effective mass (m_e) and effective height (H_e) of the equivalent SDOF system. The following equations are used for each of them.

$$\Delta_d = \sum_{i=1}^n (m_i \Delta_i^2) / \sum_{i=1}^n (m_i \Delta_i) \quad (6)$$

$$m_e = \frac{\sum_{i=1}^n (m_i \Delta_i)}{\Delta_d} \quad (7)$$

$$H_e = \sum_{i=1}^n (m_i \Delta_i H_i) / \sum_{i=1}^n (m_i \Delta_i) \quad (8)$$

where, m_i and Δ_i are the mass and displacement of the i^{th} story, respectively.

Equivalent damping for the SDOF system can be obtained through the following equation [13]:

$$\xi_{eq} = 0.05 + 0.565 \left(\frac{\mu - 1}{\mu \pi} \right) \quad (9)$$

The first term of the above equation is the 5% elastic viscous damping and the second term is the hysteretic damping, and μ is the design displacement ductility factor, and it is equal to:

$$\mu = \frac{\Delta_d}{\Delta_y} \quad (10)$$

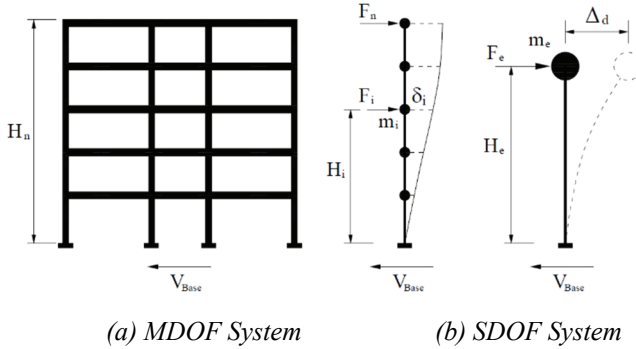


Figure 3 - Simplified model of MDOF system represented by SDOF system [55].

In this equation, Δ_y is the yield displacement of the equivalent SDOF system. For RC frame buildings with three bays (refer to Figure 3), it can be obtained using the following equation [13]

$$\Delta_y = \frac{2M_1 \theta_{y_1} + M_2 \theta_{y_2}}{2M_1 + M_2} H_e \quad (11)$$

where M_1 and M_2 are the moment contribution to the total overturning moment from outer and inner bays respectively. θ_{y_i} is the yield drift, and it is equal to:

$$\theta_{y_i} = 0.5\varepsilon_y \frac{L_{b_i}}{h_{b_i}} \quad (12)$$

In this equation, ε_y is the yield strain, which is the ratio of expected yield strength (f_{ye}) of the reinforcement over its modulus of elasticity (E_s), L_{b_i} is the length of the i^{th} bay and h_{b_i} is the depth of the beam of the i^{th} bay. It should be noted that Priestley et al. [56] recommended that f_{ye} should be taken 10% larger than characteristic yield strength (i.e. $f_{ye} = 1.1f_y$). Furthermore, in Equation (11), the values for M_1 and M_2 are not required; instead, only the ratio of them is needed. This ratio can be arbitrarily chosen, however, for the case study, since the depth of the beams is kept constant for all three bays, and it is assumed that the moment capacity of the inner and outer frames are equal, so according to the recommendation of Priestley et al. [56] this ratio is equal to:

$$\frac{M_1}{M_2} = 1 \Rightarrow M_1 = M_2 \quad (13)$$

Using this value, Equation (11) results in the following simple form:

$$\Delta_y = \frac{2\theta_{y_1} + \theta_{y_2}}{3} H_e \quad (14)$$

The design displacement response spectrum for the desired damping ($S_{D_{\xi}}$) rather than 5% elastic damping, can be obtained using the following equation [56]:

$$S_{D_{\xi}} = S_{D_{e,5}} \left(\frac{0.10}{0.05 + \xi_{eq}} \right)^{0.5} \quad (15)$$

In this equation $S_{D_{e,5}}$ is the design displacement response spectrum for 5% damping, which is equal to:

$$S_{D_{e,5}} = S_{ae}(T) \frac{T^2}{4\pi^2} \quad (16)$$

where $S_{ae}(T)$ is the elastic design acceleration response spectrum, which could be obtained by using TSC-2007 and TBEC-2018 separately. Since in the DDBD approach, displacement response spectrum is used, there must be a constant maximum displacement after reaching a specific value for the effective period, called the corner period. There is nothing mentioned about the corner period in TSC-2007, while in TBEC-2018, it is given as T_L and it is equal to 6 seconds; therefore, for TSC-2007, it is also assumed to be 6 sec. One of the reasons for

using a large period as a corner period is to adjust the design displacement spectrum to be useful for the higher value of the effective period resulting from the lower effective stiffness of the SDOF system [8]. Here, only the resultant elastic acceleration response spectrum for 5% damping has been shown in Figure 4 with design displacement response spectra for different damping values for both TSC-2007 and TBEC-2018.

From Figure 4, it can be concluded that the values for the design displacement response spectrum for TBEC-2018 are significantly smaller than the ones obtained for TSC-2007. Response spectra for TBEC-2018 are shown up to 6.5 sec, which is an arbitrary value, and the constant region for the displacement can be noticed clearly. On the other hand, for TSC-2007, it is shown up to 6 sec since, using equations provided in TSC-2007 it is not possible to obtain the constant displacement region.

Once such response spectra for the design displacement are obtained, then using design displacement (Δ_d) in the design displacement response spectrum for equivalent damping of the given figure, the corresponding effective period can be read as shown in Figure 4.

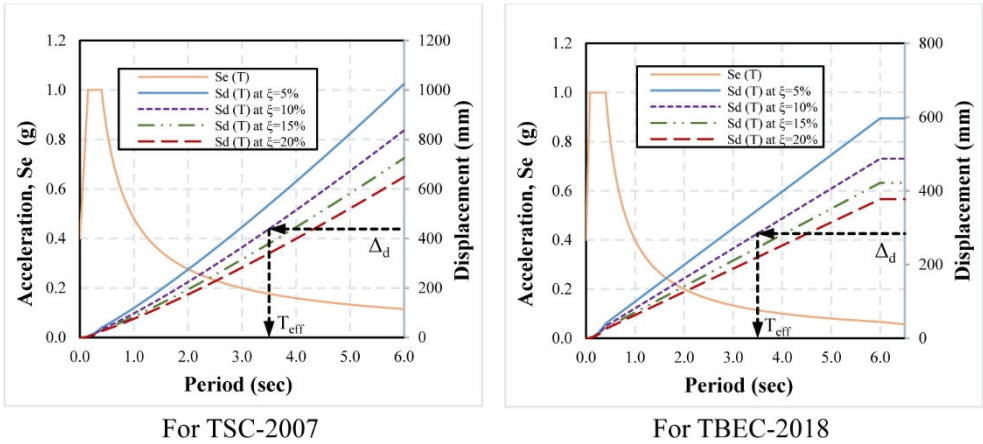


Figure 4 - Elastic acceleration (S_e) and design displacement (S_d) response spectra for different damping values.

$$\Delta_d \Rightarrow T_{eff}$$

Finally, the effective period is used to obtain effective stiffness and total base shear force as follows, respectively.

$$K_{eff} = \frac{4\pi^2}{T_{eff}^2} m_e \tag{17}$$

$$V_{Base} = K_{eff} \Delta_d \tag{18}$$

The total base shear force is then distributed up the height of the building, and lateral forces at the top of each floor are obtained using the following equation, provided by both TSC-2007 and TBEC-2018.

$$F_i = (V_{Base} - \Delta F_N) \frac{m_i H_i}{\sum_{i=1}^n m_i H_i} \quad (19)$$

where m_i is the mass of the i^{th} story. ΔF_N is the additional equivalent seismic load, acting at the top of the N^{th} floor, and it is equal to:

$$\Delta F_N = 0.0075N V_{Base} \quad (20)$$

Here, N is the total number of stories of the building (see Figure 5).

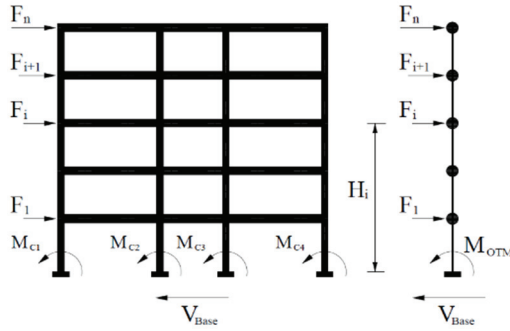


Figure 5 - Story forces and total overturning moment (M_{OTM}) [13].

The stability index (θ_Δ) is calculated by Equation (21) to see if P-Delta effects are required to be considered in the analysis. According to model code DBD12 [14], the stability index shall not exceed 0.3. If $0.1 \leq \theta_\Delta \leq 0.30$, P-Delta effects should be considered. If $\theta_\Delta > 0.30$, then the structure must be made stiffer and the calculations should be revised. Furthermore, if $\theta_\Delta < 0.1$, then there is no need to consider P-Delta effects. The base shear force is amplified (if $0.1 \leq \theta_\Delta \leq 0.30$ and will be calculated by Equation (22) [13, 55].

$$\theta_\Delta = \frac{P\Delta_{max}}{M_D} \quad (21)$$

$$V_{Base} = K_{eff} \Delta_d + C \frac{P\Delta_d}{H_e} \quad (22)$$

where M_D and Δ_{max} are total overturning moment (M_{OTM}) at the base of the structure and design displacement of the equivalent SDOF system obtained by using Equation (6), respectively [55]. P is the axial force due to gravity loads, C is a constant, and for reinforced concrete structures, $C=0.5$ is used.

$$M_{OTM} = \sum_{i=1}^n F_i H_i \quad (23)$$

Once the base shear force is distributed up the height of the building using Equation (19), then it is easy to find the story shear forces. Two different methods of structural analysis under lateral forces vector are given by Priestley et al. [13] in the DDBD approach for the determination of moment capacities at plastic hinge locations. The first one is the analysis of the frame under lateral forces based on the relative stiffness of the members, and the second one is based on the equilibrium consideration of the nodes. Here, the latter is being considered. In this method, to find the shear forces in the columns at each story, the inner columns are assumed to take twice the shear forces compared to the outer columns. To avoid the soft story mechanism of the first story, the contra flexure height for columns of the first story is considered at 0.6 of the height of that story ($0.6H_1$) from the base of the column [13]. For further discussions about how to find the internal forces in columns and beams and for discussions about capacity design principles, the reader is referred to Priestley et al. [13].

4. EVALUATION OF RESPONSE MODIFICATION FACTOR (R)

The TSDCs are based on the FBD approach and some linear elastic techniques. In most of these codes, the nonlinear behavior of structures is not considered directly in the design process; instead, their nonlinear behavior is considered by means of the response modification factor (R), which reduces the demand due to design earthquake [4, 57]. Since the design earthquake is a rare event that a structure may experience in its life cycle, to have an economical design, the structures are allowed to go under inelastic deformation and dissipate induced energy by inelastic deformation due to the design earthquake, so TSDCs handle that by R factors and properly designed seismic details. In seismic design codes, specific R factors are used for specific types of structures. R factor is the ratio of the maximum elastic base shear force (V_e) of a structure obtained through elastic analysis to its maximum inelastic base shear force (V_u) obtained through inelastic analysis. R factor could be evaluated for a designed structure, for which alternative formulations are proposed in the literature. The following equation widely used in research works, such as [58–65], is used in this study.

$$R = R_{\Omega} R_{\mu} \quad (24)$$

In this equation, R_{Ω} is the overstrength factor and R_{μ} is the ductility factor, given as follows:

$$R_{\Omega} = \frac{V_y}{V_d} \quad (25)$$

$$R_{\mu} = \left(\frac{\mu - 1}{\Phi} \right) + 1 \quad (26)$$

$$\mu = \frac{u_{max}}{u_y} \quad (27)$$

$$\Phi = 1 + \frac{1}{10T - \mu T} - \frac{1}{2T} e^{-1.5(\ln T - 0.6)^2} \quad (28)$$

where V_y is the base shear force at the yield point (Figure 6) which cannot be less than the design base shear force (V_d), u_{max} is the maximum top displacement of the structure that it can go for, and u_y is the displacement at the yield strength of the structure, μ is global ductility ratio, Equation (27), and Φ is the factor which depends on soil condition, and for rock type soil it can be calculated through Equation (28), T is the fundamental period of the structure. Equations (26) and (28) are suggested by Miranda and Bertero [66]. The concept of the response modification factor is illustrated in Figure 6 (in the figure $\Delta_y = u_y$ and $\Delta_u = u_{max}$).

For evaluation of the R-value, the capacity curve, obtained through pushover analysis of the structure, is approximated by a bilinear curve to obtain a clear yield point (which corresponds to V_y Figure 7). Different methods exist for this purpose. One of the methods used in this study is called the equal-energy method, which assumes that the areas enclosed by the pushover curve above and below the bilinear curve are equal ($Area_1 \cong Area_2$).

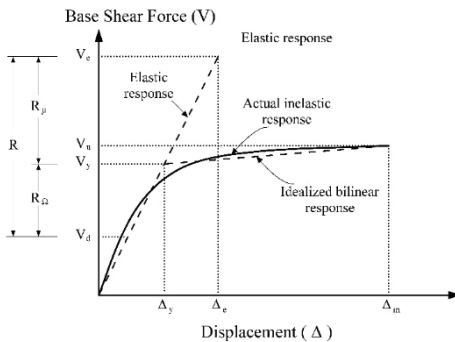


Figure 6 - Base shear force vs roof displacement relationship [58].

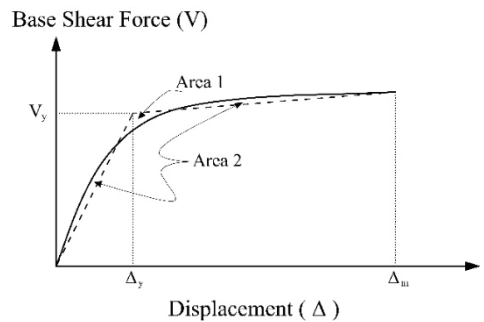


Figure 7 - Bilinear approximation of the capacity curve [67].

5. ENDURANCE TIME METHOD

A hypothetical shaking-table test could be used to explain the concept of the Endurance Time (ET) method. As shown in Figure 8, the structures are located on shaking-table and loaded with an intensifying artificial dynamic excitation. The aim is to determine the relative performance of the three structures under dynamic excitation [32].

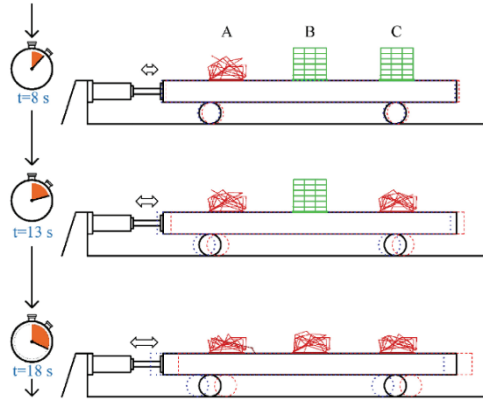


Figure 8 - Hypothetical shaking-table test [32].

The response of the structures is tracked during the hypothetical shaking-table test. The behavior of the structures shifts gradually from linear elastic behavior to nonlinear inelastic behavior, experiencing some damage states, and finally, collapse will occur as the amplitude of the ET excitation increases with time. The results of the hypothetical shaking-table test are given in terms of the ET curves, which show the relation between ET and EDPs, e.g., maximum IDR. The main advantage of the ET method over the conventional NTHA procedure utilizing ground motions is that the computational time for analysis is reduced significantly [68]. It is worth mentioning that the actual EDPs and final design, obtained using the ET method, should be verified by conducting more precise procedures, e.g., IDA and cloud analysis methods [69, 70].

In contrast to the typical time history analysis, which uses real Ground Motion (GMs) or artificially generated motions, the ET method utilizes the ETEFs, which are the main component of the ET method, and thus directly affects the results. The ETEFs are acceleration functions for which the intensity increases with time, and from zero to each time corresponds to a specific seismic hazard level. They are created such that to induce suitable responses in structures as compared to GMs [40]. In this study, the ETA40lc series of ETEFs are used that are generated by Mashayekhi et al. (2018) [40] using the FEMAP695 far-field record set (22 real GM records). For the simulation of this series of ETEFs, the consistency of the ground motion duration has been included directly in the generation process. This is because structural responses could be influenced by ground motion duration significantly [71–74]. In addition, since the ETA40lc series of ETEFs follows an exponentially intensifying profile that is consistent in cumulative absolute velocity (CAV) when compared to conventional GM scaling to match desired intensity. Some research works showed that the

CAV could also be used as an alternative for the Arias Intensity (AI) [75–77] to evaluate the motion duration’s effect on structural response [78]. To this end, the CAV has been included in the generation process of the ETA40lc series, and it has been selected as an IM to reflect the impact of duration [40]. The target acceleration response spectrum of the ETEFs can be defined as follows:

$$S_{ac}(t, T) = g(t) \times S_a^{\text{target}}(T) \quad (29)$$

where, $S_a^{\text{target}}(T)$ is GMs target acceleration spectrum as the average acceleration response spectrum of GMs. The records of the ETA40lc series have been optimized to fit the average acceleration spectrum, average displacement spectrum, and average CAV of the first components of the FEMAP695 far-field GM set. These GMs are recorded on soft rock, stiff sites, and shallow crustal sites. Site-to-sources distances are at least 10 km, and the magnitudes of the events are larger than 6.5. The peak ground velocity of each individual record is used for normalization while generating the ETA40lc series. To this end, Mashayekhi et al. (2018) [40] used the procedure of the FEMAP695 [79] in their study. Because of inherent differences in magnitude, source type, and site condition, there is unwarranted variability between records; thus, normalization is used considering peak ground velocity to eliminate them while retaining inherent aleatory variability for anticipating seismic response assessment [42, 79]. In Figure 9, $S_a^{\text{target}}(T)$ related to these GMs are shown. $g(t)$ is the intensifying profile which controls the shape of increasing acceleration spectra in time [40].

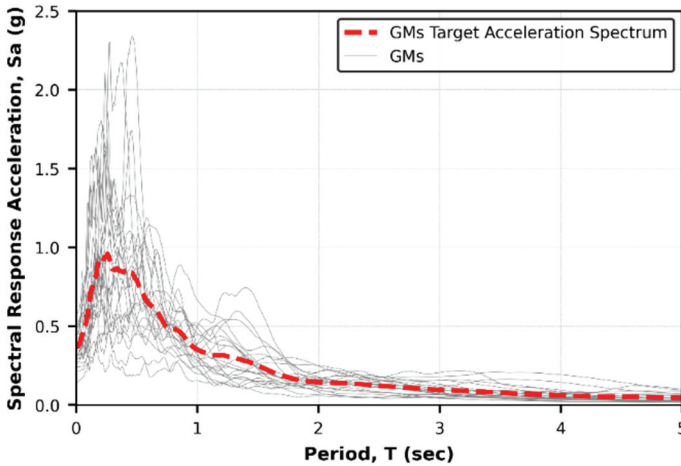


Figure 9 - Target acceleration spectrum of first components of FEMAP695 far-field GM set

Figure 10 shows the ETA40lc01 accelerogram and the comparison of its acceleration response spectra at different times of excitation with target response spectra. Three excitation functions of the ETA40lc series are used in this study to reduce the effects of random scatter

in the results, as recommended in research work by Estekanchi et al. [80]. The target times of these excitation functions are calculated in such a way that first, the GMs target acceleration spectrum is placed above the code spectrum in the range of $0.2T$ to $1.5T$ (T is the fundamental period of the structure), and second, the average acceleration response spectrum of ETA40lc01-03 is matched with the scaled GMs target acceleration spectrum in the same interval of $0.2T$ to $1.5T$. The variation of the corresponding hazard return period with the target time in ET analysis and structural period in this study is shown in Figure 11.

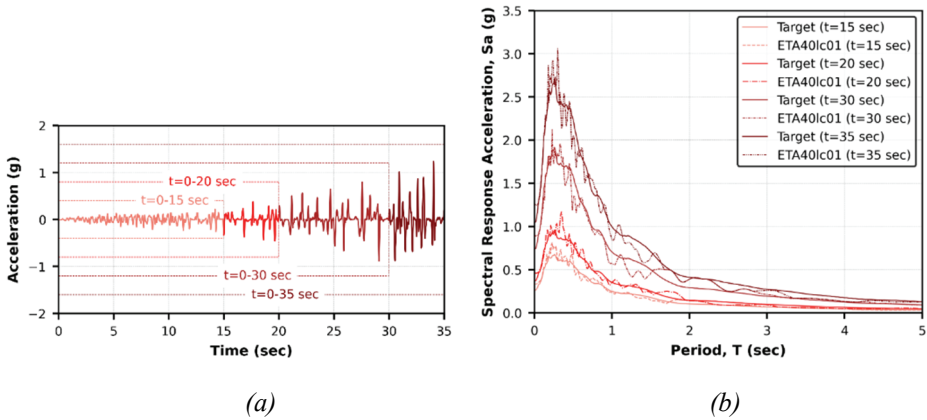


Figure 10 - (a) ETA40lc01 accelerogram, (b) Acceleration response spectra at different times of excitation.

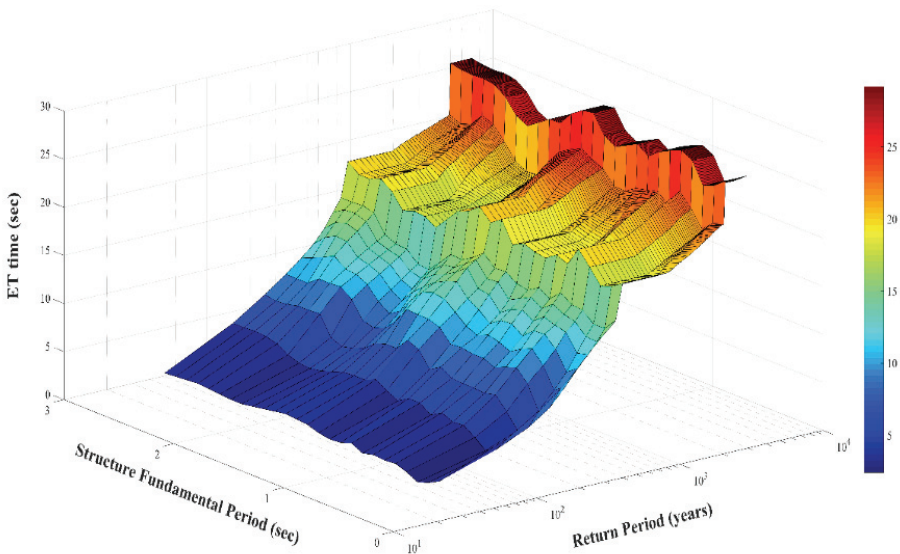


Figure 11 - Return period vs. target time in ET analysis and structural period.

6. STRUCTURAL DESIGN

6.1. Seismic Design Codes

Four special moment-resisting RC frames are selected to demonstrate the DDBD approach. They are related to commercial office buildings, similar in terms of the plan, while different in terms of the number of stories (three-, five-, eight-, and 12- story buildings). It is assumed that the structures are located in Düzce province, in the north of Türkiye. The necessary parameters for estimating the acceleration response spectrum for TBEC-2018 were obtained, such as S_S and S_1 . Since the location is close to the North Anatolian fault, which is an active fault, according to TSC-2007, seismic zone 1 with $A_0 = 0.4$ is chosen. The site class used in this study is Z1 according to TSC-2007, which corresponds to ZB given by TBEC-2018 [52]. The compressive strength of the concrete used here is 25 MPa, and the elasticity modulus of the concrete is assumed to be equal to 3.1×10^4 MPa. The yield strength of the steel reinforcement is taken as 420 MPa, and its modulus of elasticity is equal to 2×10^5 MPa. The selected frames in each case have the highest gravitational loads on them (i.e., the gravity load is maximum on the chosen frame in each case), and each has three bays, the outer bays of the frames are larger than the inner bay. Cross-sectional sizes for each frame are provided in Table 1. Elevation of frames with their vertical and horizontal dimensions is given in Figure 12.

6.2. DDBD Approach

The DDBD approach is applied to the frames in compliance with TSC-2007 and TBEC-2018, and base shear forces are obtained. The detailed design for the given frames with specified cross-sectional sizes is carried out only for the base shear forces obtained through the DDBD in compliance with TSC-2007. Since the base shear forces obtained through the DDBD as per TBEC-2018 are much smaller, cross-sectional sizes are changed for the frames, and the DDBD in accordance with TBEC-2018 has been applied once again, and the base shear forces are obtained. In this case, cross-sectional sizes are given in Table 2, and it should be noted that for detailed design, TSC-2007 and TBEC-2018, together with TS-500, are used. Then, the R factor is evaluated for each frame designed in both cases from the results obtained through nonlinear static pushover analysis.

Table 1 - Designed sections for the studied RC frames

Frame	Story-Level	Member Size		
		Beams	Exterior Columns	Interior Columns
3-Story	1-3	35x50 cm	40x40 cm	40x40 cm
5-Story	1-3	35x60 cm	50x50 cm	50x50 cm
	4-5	35x60 cm	45x45 cm	45x45 cm
8-Story	1-5	35x60 cm	60x60 cm	60x60 cm
	6-8	35x60 cm	50x50 cm	50x50 cm
12-Story	1-8	35x60 cm	70x70 cm	70x70 cm
	9-12	35x60 cm	60x60 cm	60x60 cm

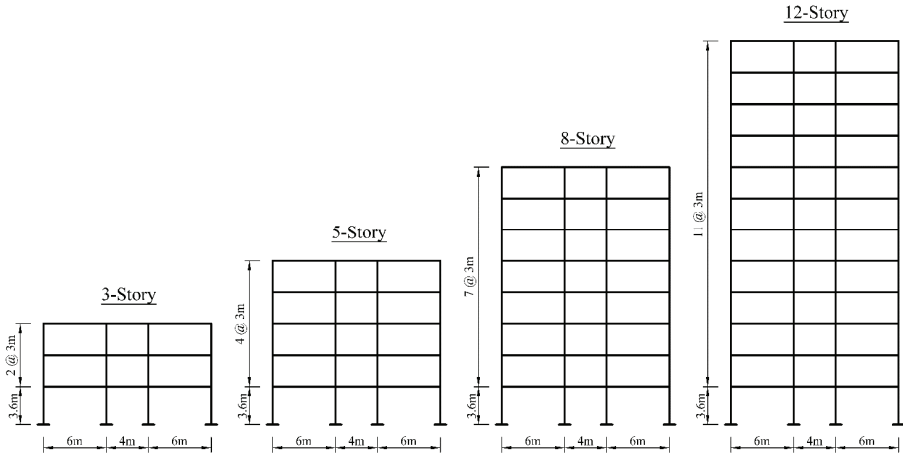


Figure 12 - Elevation of frames with their vertical and horizontal dimensions.

6.3. Discussion of the Results

The results obtained for the DDBD approach in accordance with both TSC-2007 and TBEC-2018, for some important parameters, are tabulated in Table 3 for the same frames, i.e., having the same cross-sectional sizes for columns and beams in both cases. From Table 3, it can be seen that up to equivalent damping, the results are the same in both cases, while after that, since TSC-2007 and TBEC-2018 are involved, the results are different. The ductility demands of the frames are slightly changing with respect to the height of the frames in both cases. The design displacement ductility (μ) is slightly reducing with the increase in the number of stories (in the case of three-story, since the depth of the beams is 50cm while in other cases it is 60cm; thus, the μ is smaller than the one for five and eight-story frames) in both cases. A similar conclusion can be made regarding equivalent damping. For frames with the same cross-sectional sizes of the beams, the stiffness of the frames is reducing significantly with the increasing number of stories. Stability indices, in the case of DDBD in accordance with TSC-2007 are slightly changing, while in accordance with TBEC-2018 the changes are significant. Finally, the changes in base shear forces obtained for frames through the DDBD approach in accordance with TSC-2007 are significant compared to the ones obtained for frames in accordance with TBEC-2018.

Tables 3-5 show the base shear forces obtained through the DDBD in compliance with TSC-2007 and TBEC-2018 and the ones obtained through TSC-2007 and TBEC-2018 by the ELF method for different R factors, respectively. These results are also shown in Figure 13. It should be noted that while modeling frames, the beams are assumed to be axially rigid members. From Table 4 and Figure 13a, it can be concluded that for the three-story frame, the base shear force obtained through the DDBD as per TSC-2007 is slightly smaller than the one obtained for the same frame through TSC-2007 by the ELF method for $R=4$. On the other hand, for the remaining frames, the DDBD approach estimates higher values of the base shear forces compared to the ones obtained for the same frames through TSC-2007 by the ELF method for $R=4$.

Table 2 - Re-designed sections for the studied RC frames through TBEC-2018

Frame	Story-Level	Member Size		
		Beams	Exterior Columns	Interior Columns
3-Story	1-3	25x50 cm	35x35 cm	35x35 cm
5-Story	1-5	30x50 cm	40x40 cm	40x40 cm
8-Story	1-8	30x50 cm	50x50 cm	50x50 cm
12-Story	1-8	30x50 cm	55x55 cm	55x55 cm
	8-12	30x50 cm	30x50 cm	30x50 cm

Table 3 - Initial design values of frames obtained through DDBD approach.

	According to TSC-2007				According to TBEC-2018			
	3-Story	5-Story	8-Story	12-Story	3-Story	5-Story	8-Story	12-Story
Drift Limit, θ_d (%)	2	2	2	2	2	2	2	2
Design Displacement, Δ_d (mm)	145.08	185.39	278.28	403.41	145.08	185.39	278.28	403.41
Effective height, H_e (m)	7.25	10.86	16.57	24.24	7.25	10.86	16.57	24.24
Effective Mass, m_e (ton)	163.17	293.40	473.37	731.85	163.17	293.40	473.37	731.85
Yield Displacement, Δ_y (mm)	89.37	111.54	170.11	248.82	89.37	111.54	170.11	248.82
Design Displacement Ductility, μ	1.62	1.66	1.64	1.62	1.62	1.66	1.64	1.62
Equivalent Damping, ξ_{eff} (%)	11.91	12.16	11.99	11.89	11.91	12.16	11.99	11.89
Effective Period, T_{eff} (sec)	1.464	1.807	2.525	3.432	1.898	2.444	3.649	5.275
Effective Stiffness, K_{eff} (kN/m)	3005.26	3546.03	2932.09	2453.20	1788.48	1939.77	1403.22	1038.36
Base Shear Force, V_{Base} (kN)	436.00	657.41	815.94	989.65	259.47	359.62	390.49	418.88
Stability Index, θ_{Δ}	0.09	0.09	0.12	0.15	0.16	0.17	0.25	0.32
Final Base Shear Forces, V_{Base} (kN)	436.00	657.41	868.01	1070.82	280.22	391.39	442.56	491.32

However, a different conclusion can be made about the results obtained for base shear forces for the frames through the DDBD in compliance with TBEC-2018 and the ones obtained for the same frames through TBEC-2018 by the ELF method. As it is evident from Table 5 and Figure 13, the base shear force obtained for the three-story frame through the DDBD in accordance with TBEC-2018 is very close to the value obtained through TBEC-2018 by the ELF method for $R=7$, while for the remaining frames base shear forces obtained through the DDBD in accordance with TBEC-2018 are close enough to the ones obtained through TBEC-2018 by the ELF method for $R=6$.

Another conclusion could be made regarding the results obtained through the TSC-2007 and TBEC-2018 by the ELF method. As can be seen from Tables 4 and 5, for the frames with the lower number of stories, both TSC-2007 and TBEC-2018 give close results; however, by increasing the number of stories, the differences in the results are significantly increasing. One of the reasons for such difference is due to the design displacement response spectra, which could be obtained from acceleration response spectra provided in both TSC-2007 and TBEC-2018.

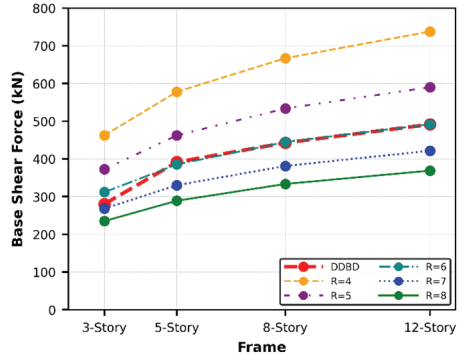
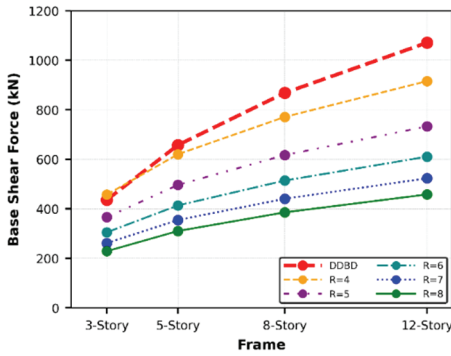
As can be seen from Figure 4, the design displacement response spectrum for TSC-2007 is significantly larger than the one for TBEC-2018 for the same damping ratio and identical effective period. For example, for 5% damping at 6sec for TSC-2007, the design displacement is equal to around 1050 mm, while for TBEC-2018, it is equal to around 600 mm.

Table 4 - Base shear forces (kN) obtained through DDBD approach and ELF method based on TSC-2007

Number of Stories	DDBD	TSC-2007 by ELF method				
		R=4	R=5	R=6	R=7	R=8
3	436.00	457.27	365.81	304.85	261.30	228.63
5	657.41	620.28	496.23	413.52	354.45	310.14
8	868.01	770.87	616.70	513.92	440.50	385.44
12	1070.82	915.64	732.51	610.43	523.22	457.82

Table 5 - Base shear forces (kN) obtained through DDBD approach and ELF method based on TBEC-2018.

Number of Stories	DDBD	TBEC-2018 by ELF method				
		R=4	R=5	R=6	R=7	R=8
3	280.22	462.34	372.35	311.68	268.01	235.08
5	391.39	577.70	462.16	385.13	330.11	288.85
8	442.56	666.85	533.48	444.56	381.06	333.42
12	491.32	737.55	590.04	491.70	421.45	368.77



(a) (b)
 Figure 13 - Comparison of base shear forces obtained through DDBD approach and ELF method based on: (a) TSC-2007 and (b) TBEC-2018.

As mentioned earlier that, the base shear forces obtained for the frames through the DDBD in accordance with TBEC-2018 were very small (see Tables 4 and 5); therefore, cross-sectional dimensions for columns and beams are reduced. The DDBD approach in compliance with TBEC-2018, is once again applied on frames with smaller cross-sectional dimensions for columns and beams, and the base shear forces are obtained. The results of some important parameters are shown in Table 6. Note that for the 12-story frame, according to TBEC-2018, the stability index has exceeded the limit $\theta_{\Delta} = 0.32 > 0.30$ (see Table 3).

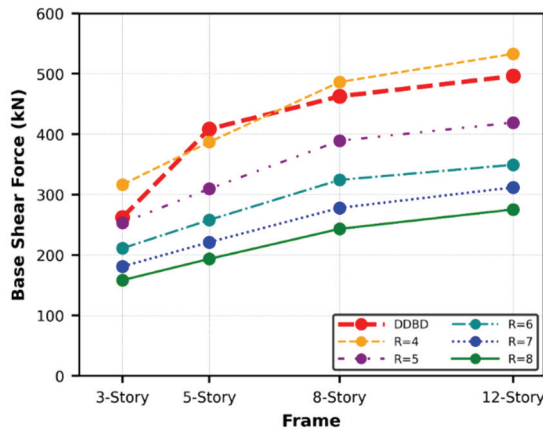


Figure 14 - Comparison of base shear forces obtained through DDBD approach and ELF method based on TBEC-2018 for the re-designed frames.

However, from equation (21), it is evident that the gravity loads also affect the stability index; thus, by reducing the gravity loads, the stability index may be reduced. With the reduction in

the cross-sectional dimensions, the gravity load is also reduced, which results reduction in the stability index (see Table 6, $\theta_{\Delta} = 0.28 < 0.30$). In addition, the same frames are analyzed through TBEC-2018 by the ELF method for different values of R , and the base shear forces are obtained. The results are tabulated in Table 7 together with the base shear forces obtained through the DDBD in compliance with TBEC-2018 and shown in Figure 14.

Table 6 - Initial design values of frames obtained through the DDBD approach for the re-designed frames.

	DDBD Results According to TBEC-2018			
	3-Story	5-Story	8-Story	12-Story
Drift Limit, θ_d (%)	2	2	2	2
Design Displacement, Δ_d (mm)	144.96	185.54	279.34	405.77
Effective height, H_e (m)	7.25	10.87	16.64	24.40
Effective Mass, m_e (ton)	154.01	270.43	438.37	648.51
Yield Displacement, Δ_y (mm)	89.30	133.96	205.02	300.65
Design Displacement Ductility, μ	1.62	1.39	1.36	1.35
Equivalent Damping, ξ_{eff} (%)	11.91	10.00	9.78	9.66
Effective Period, T_{eff} (sec)	1.897	2.286	3.417	4.943
Effective Stiffness, K_{eff} (kN/m)	1689.66	2042.54	1482.04	1047.83
Base Shear Force, V_{Base} (kN)	244.94	378.98	413.99	425.18
Stability Index, θ_{Δ}	0.14	0.15	0.22	0.28
Final Base Shear Forces, V_{Base} (kN)	262.20	408.53	462.54	496.25

Table 7 - Base shear forces (kN) obtained through DDBD approach and ELF method based on TBEC-2018 for the re-designed frames.

Number of Stories	DDBD	TBEC-2018 by ELF method				
		R=4	R=5	R=6	R=7	R=8
3	262.20	316.58	253.26	211.05	180.90	158.29
5	408.53	386.95	309.56	257.97	221.12	193.48
8	462.54	486.32	389.06	324.21	277.90	243.16
12	496.25	532.99	419.19	349.33	311.88	275.35

From Table 7 and Figure 14, it can be concluded that the depth of the beams has a significant effect on design displacement ductility, and with the increase in the depth of the beam, the design displacement ductility increases (refer to Equations (10)-(14)). As a consequence, increase in effective period and reduction in base shear force could be witnessed.

7. ANALYSIS AND RESULTS

7.1. Pushover Analysis and Results

The frames are designed in detail for the base shear forces obtained through the DDBD in accordance with TSC-2007 and TBEC-2018 (provided in Tables 4 and 7) by using TS-500. The capacity design principle is used to obtain the beam sway mechanism (i.e., strong-column weak-beam mechanism). In nonlinear static pushover analysis, horizontal forces are distributed up the height of the frames as inverse triangular. In this section, the results of the nonlinear static pushover are presented.

Nonlinear static pushover analysis is performed on all frames in both cases, and the results for the sway mechanism and pushover curves are shown. The results of the beam sway mechanism shown in Figure 15 for the frames designed for the base shear forces obtained through the DDBD approach in accordance with TSC-2007 are satisfactory. The capacity curves for these frames along with the idealized bilinear curves, are shown in Figure 16. The results of the beam sway mechanism shown in Figure 17 for the frames designed for the base shear forces obtained through the DDBD approach in accordance with TBEC-2018 are also satisfactory. The capacity curves for these frames along with the idealized bilinear curves, are shown in Figure 18. From Figures 15-18, it can be observed that the initial objective of the design of the frames, which is LS performance level, is satisfied for all frames, even for higher values of base shear forces than the design base shear forces.

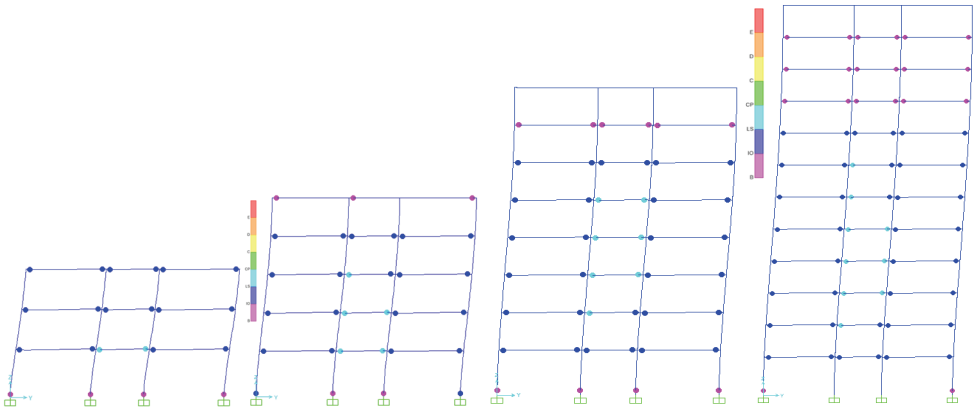


Figure 15 - Sway mechanisms obtained through pushover analysis for frames designed by DDBD in accordance with TSC-2007,

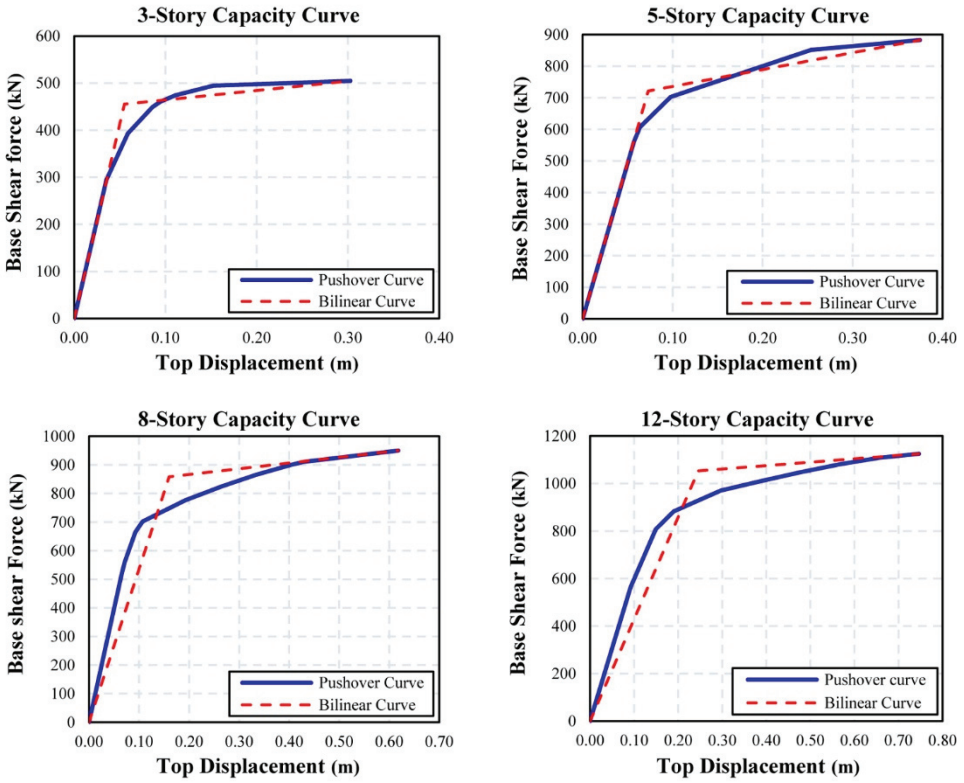


Figure 16 - Capacity curves obtained through pushover analysis for frames designed by DDBD in accordance with TSC-2007.

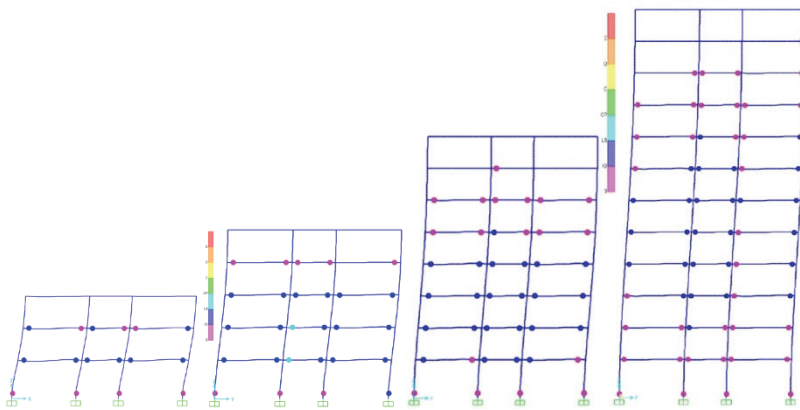


Figure 17 - Sway mechanisms obtained through pushover analysis for frames designed by DDBD in accordance with TBEC-2018.

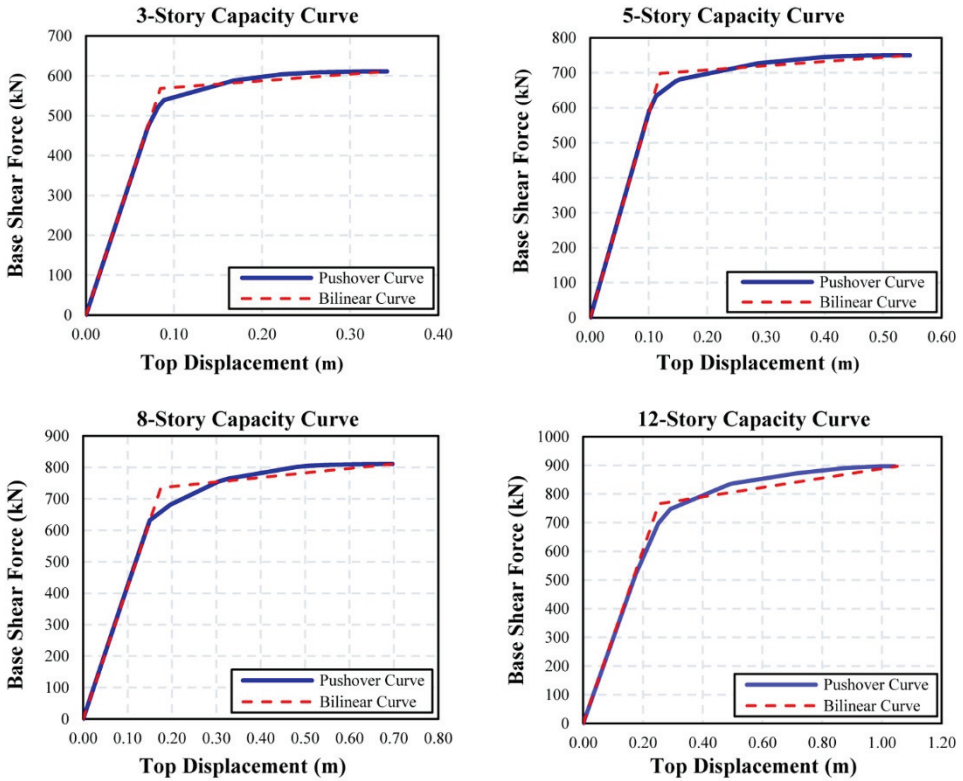


Figure 18 - Capacity curves obtained through pushover analysis for frames designed by DDBD in accordance with TBEC-2018.

The results for some of the important parameters together with the evaluated R values for the designed frames in both cases are tabulated in Table 8.

From the table, it can be observed that for the case in which frames are designed through the DDBD approach in accordance with TSC-2007, overstrength factors for all frames are around one. They are just above one for 3- and 5-story frames, while for the 8- and 12-story frames, they are exactly one. This is because the yield strength of the structure should not be less than the design strength of the structure; thus, the yield strength of the structure is kept at least equal to the design strength. However, for the case in which frames are designed through the DDBD approach based on TBEC-2018, overstrength factors for all frames are larger than one. In addition, generally, in both cases, the R values are reduced with an increase in the number of stories. Finally, from the table, it can be seen that RC frames designed using the DDBD approach based on TBEC-2018 provide higher R -value values than those designed using the DDBD approach based on TSC-2007. This is because of the overstrength factors, which for the cases designed through the DDBD approach with respect to TBEC-2018 are much larger than for the case of frames designed using the DDBD approach with respect to TSC-2007.

Table 8 - Evaluated values of R for designed frames with some important parameters.

Parameters	DDBD in Accordance with TSC-2007				DDBD in Accordance with TBEC-2018			
	3-Story	5-Story	8-Story	12-Story	3-Story	5-Story	8-Story	12-Story
V_d (kN)	436.00	657.41	858.83	1053.00	262.20	408.53	462.54	496.25
V_y (kN)	455.46	721.30	858.83	1053.00	568.20	698.14	735.46	765.72
V_u (kN)	504.61	882.99	950.15	1124.77	611.19	749.73	811.04	896.94
u_y (m)	0.0550	0.0728	0.1600	0.2455	0.0846	0.1197	0.1752	0.2533
u_{max} (m)	0.3027	0.3749	0.6180	0.7467	0.3418	0.5458	0.6970	1.0517
R_{Ω}	1.0446	1.0972	1.00	1.00	2.1670	1.7089	1.5901	1.5430
μ	5.5061	5.1486	3.8626	3.0415	4.0412	4.5595	3.9777	4.1523
T (sec)	0.7417	0.8783	1.2418	1.7741	0.8407	1.1357	1.6686	2.4758
Φ	1.0993	0.9786	0.8082	0.7995	0.9572	0.8470	0.8033	0.9027
R_{μ}	5.0989	5.2393	4.5417	3.5535	4.1771	5.2026	4.7067	4.4922
R	5.3265	5.7485	4.5417	3.5535	9.0518	8.8907	7.4839	6.9858

7.2. ET Analysis and Results

To compare the results obtained by the DDBD approach based on two Turkish seismic codes by dynamic analyses, the ET method is used due to its ability to decrease computational efforts and provide reasonable estimates of structural responses. To consider the impact of ground motion duration on the structural responses, the ETA40lc series of excitation functions are used for which the cumulative absolute velocity (CAV) has been included in its generation process. Three earthquake hazard levels having the probability of exceedance 50%, 10%, and 2% in 50 years with 72, 475, and 2475 years of return periods are considered.

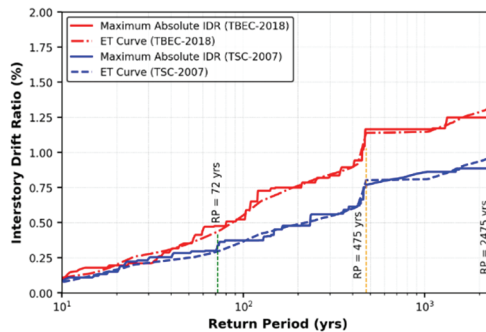


Figure 19 - Performance curve of 8-story RC frame designed by the DDBD approach in accordance with TSC-2007 and TBEC-2018.

According to the way previously stated, the target times of these excitation functions are also calculated for each frame corresponding to these hazard levels. The ET performance curve for eight-story frames is shown in Figure 19. Since the structures designed by the DDBD approach have different periods for TSC2007 and TBEC2018, the times are mapped to return periods. In this way, it becomes simpler to interpret the differences in the IDR results. As shown in the figure, TBEC-2018 exhibits higher IDRs values than TSC-2007 at various hazard levels. This confirms the results of pushover analysis as well.

The average values of maximum base shear forces of each frame at different hazard levels under ETA40lc01-03 are tabulated in Table 9 for the DDBD approach based on TSC-2007 and TBEC-2018. From the table, it can be concluded that as the number of stories increases, the base shear force is also increasing for all cases of hazard levels.

Table 9 - Average values of maximum base shear forces (kN) obtained from three ET analyses.

Number of Stories	TSC-2007			TBEC-2018		
	50%/50 yrs	10%/50 yrs	2%/50 yrs	50%/50 yrs	10%/50 yrs	2%/50 yrs
3	362.682	509.466	662.841	264.116	562.447	596.492
5	436.309	796.567	934.156	323.175	751.028	786.500
8	530.943	872.270	1161.959	335.760	835.601	935.933
12	544.646	1121.363	1477.376	380.879	878.117	1121.882

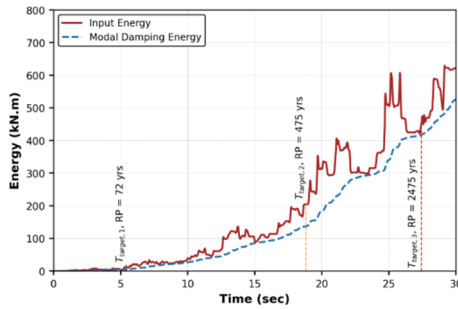
The average values of input energy and modal damping energy at target times corresponding to different hazard levels are tabulated in Table 10 and Table 11, respectively. Figure 20 shows the input and modal damping energies of the eight-story RC frame designed by the DDBD approach in accordance with TSC-2007 and TBEC-2018, obtained from ET analysis for the ETA40lc01 excitation function. In this figure, the target times for different hazard levels used in this study are also shown.

Table 10 - Average values of input energy (kN,m) at target times corresponding to different hazard levels

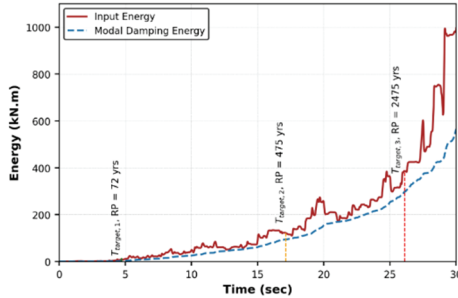
Number of Stories	TSC-2007			TBEC-2018		
	50%/50 yrs	10%/50 yrs	2%/50 yrs	50%/50 yrs	10%/50 yrs	2%/50 yrs
3	8.717	130.734	310.073	7.469	113.040	318.338
5	9.016	152.427	460.622	7.622	127.937	449.818
8	13.909	169.816	565.449	10.846	134.214	579.328
12	15.286	248.219	759.461	13.244	199.886	581.085

Table 11 - Average values of modal energy (kN.m) at target times corresponding to different hazard levels

Number of Stories	TSC-2007			TBEC-2018		
	50%/50 yrs	10%/50 yrs	2%/50 yrs	50%/50 yrs	10%/50 yrs	2%/50 yrs
3	5.742	94.345	277.810	4.094	74.787	256.388
5	5.936	119.810	406.166	4.298	96.019	344.250
8	7.719	132.585	477.114	4.436	104.832	373.628
12	8.071	172.255	582.258	6.853	98.679	252.792



(a)



(b)

Figure 20 - Input and modal damping energy for 8-story frame under *ETA40lc01*: TSC-2007 and (b) TBEC-2018.

In Figure 21, maximum IDRs resulting from *ETA40lc01-03* excitation functions and their averages for frames designed by the DDBD approach in compliance with TSC-2007 are shown for three hazard levels used in this study. Whereas Figure 22 compares the results of average maximum IDRs for the frames designed by the DDBD approach based on TSC-2007 and TBEC-2018 for three hazard levels used in this study. From this figure, it is evident that in all cases, TBEC-2018 gives higher IDR values with respect to TSC-2007, except for the case of 3-story frame at lower hazard level with the return period of 72 years.

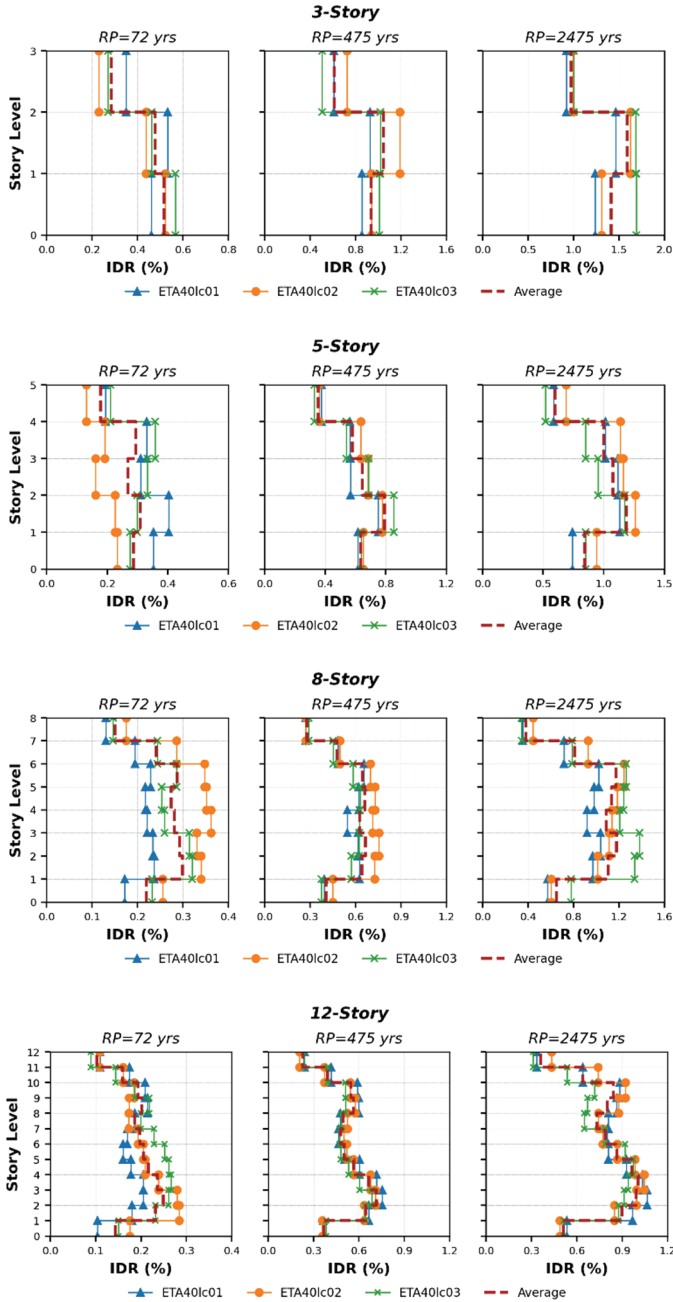


Figure 21 - IDR obtained through ET analysis for frames designed by DDBD in accordance with TSC-2007.

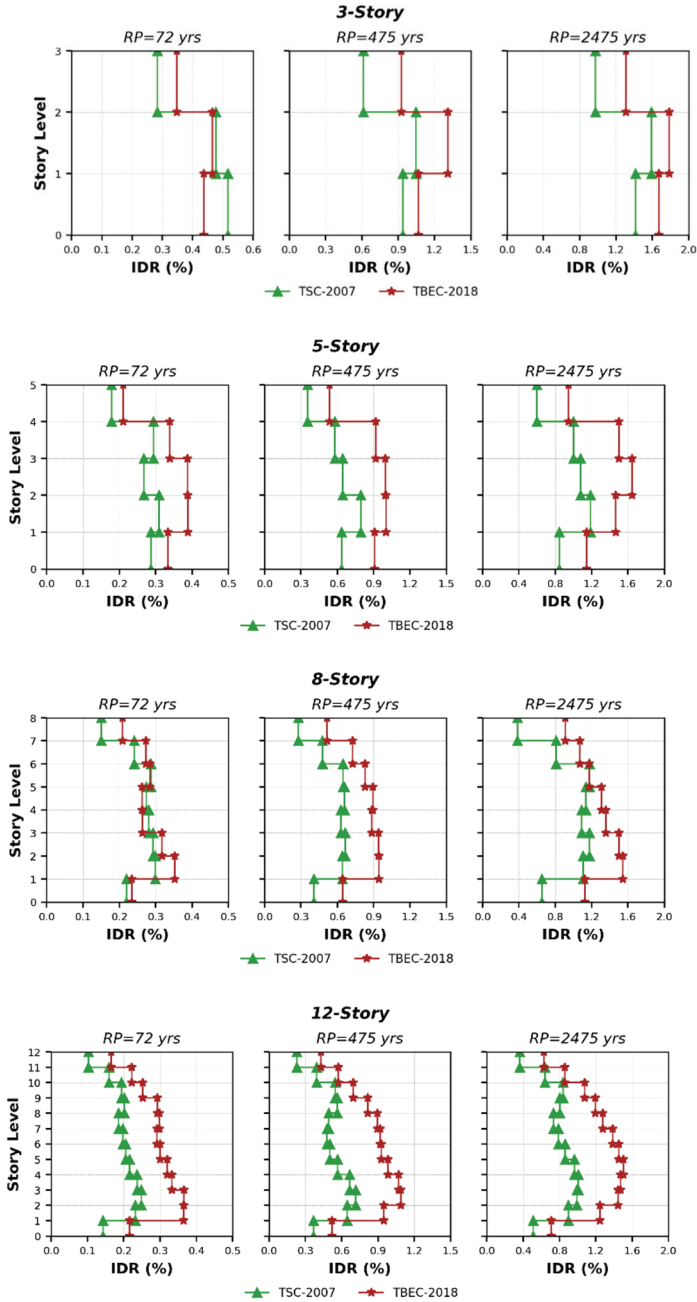


Figure 22 - Comparison of IDR obtained through ET analysis for frames designed by DDDB approach in accordance with TSC-2007 and TBEC-2018.

The difference percentage between maximum IDR, base shear force, input energy, and modal damping energy, obtained by the ET method between TSC-2007 and TBEC-2018, are tabulated in the following table.

Table 12 - Difference (%) of the results obtained by ET method between TSC-2007 and TBEC-2018

Number of Stories	Maximum IDR			Base Shear Force		
	50%/50 yrs	10%/50 yrs	2%/50 yrs	50%/50 yrs	10%/50 yrs	2%/50 yrs
3	10.47	22.37	11.55	31.45	9.89	10.54
5	22.92	23.45	32.42	29.79	5.89	17.16
8	16.50	34.55	26.83	45.04	4.29	21.55
12	38.23	41.15	39.79	35.39	24.33	27.35
	Input Energy			Modal Damping Energy		
3	15.42	14.52	2.63	33.52	23.13	8.02
5	16.76	17.47	2.37	32.02	22.05	16.50
8	24.74	23.42	2.42	54.02	23.38	24.33
12	14.31	21.57	26.61	16.31	54.31	78.91

8. SUMMARY AND CONCLUSIONS

In this paper, the DDBD approach, which is a performance-based design approach, has been applied to multi-story RC moment-resisting frames in accordance with the Turkish seismic design codes of TSC-2007 and TBEC-2018. The frames were also analyzed through TSC-2007 and TBEC-2018 by the ELF method, and the base shear forces were obtained. These base shear forces were compared with the ones obtained through the DDBD approach. The ET method is a time history-based procedure for seismic evaluation of structures under intensifying dynamic excitations aided to judge their performance at different intensity levels. Because of the ability of the ET method to diminish computational efforts and provide reasonable estimates of structural responses, it was also employed in this study to compare the results acquired by the DDBD approach on the basis of two Turkish seismic design codes.

The main findings of this research are summarized as follows:

- It was found that the DDBD approach in accordance with TSC-2007 gives higher base shear forces compared to the DDBD approach based on TBEC-2018 for frames with the same cross-sectional dimensions of the members.
- The analysis results obtained for the frames according to TSC-2007 and TBEC-2018 by the ELF method were also compared, and it was found that TBEC-2018 gives lower values of base shear forces compared to TSC-2007 for different values of R .

- After designing the frames, pushover analysis was implemented for performance assessment purposes. The beam-sway mechanism, i.e., the strong-column weak-beam concept, was satisfied for all frames in both cases.
- The results from pushover analysis also showed that frames designed through the DDBD approach in accordance with TSC-2007 give R values between 5.75 to 3.55, while the ones designed using the DDBD approach according to TBEC-2018 give R values between 6.99 to 9.05. It was also observed that with the increase in the number of stories, in general, the R values decrease in both cases.
- The ET performance curves of RC frames indicate that structures designed by the DDBD approach in accordance with TBEC-2018 exhibit higher IDRs values than TSC-2007 at various hazard levels.
- The ET analysis results showed that the DDBD approach, in accordance with TSC-2007, shows higher values for base shear force, input energy, and modal damping energy for all frames, compared to the DDBD approach as per TBEC-2018.
- The differences in the results between two Turkish seismic design codes obtained by the ET method were also calculated. It was observed that the differences in the results have various trends for the EDPs at three hazard levels used in this study.

References

- [1] Zou, X.K., Teng, J.G., De Lorenzis, L., Xia, S.H.: Optimal performance-based design of FRP jackets for seismic retrofit of reinforced concrete frames. *Compos. Part B Eng.* 38, 584–597 (2007). <https://doi.org/10.1016/j.compositesb.2006.07.016>
- [2] FEMA-445: Next-Generation Performance-Based Seismic Design Guidelines: Program Plan for New and Existing Buildings. Prepared for Federal Emergency Management Agency: Washington, DC, USA by Applied Technology Council, August 2006 (2006)
- [3] FEMA-P-58-1: Seismic performance assessment of buildings: Volume 1 – Methodology. , USA (2018)
- [4] Kalapodis, N.A., Papagiannopoulos, G.A., Beskos, D.E.: A comparison of three performance-based seismic design methods for plane steel braced frames. *Earthq. Struct.* 18, 27–44 (2020). <https://doi.org/10.12989/eas.2020.18.1.027>
- [5] Chopra, A.K., Goel, R.K.: Direct displacement-based design: Use of inelastic vs. Elastic design spectra. *Earthq. Spectra.* 17, 47–64 (2001). <https://doi.org/10.1193/1.1586166>
- [6] Moehle, J.P.: Displacement-Based Design of RC Structures Subjected to Earthquakes. *Earthq. Spectra.* 8, 403–428 (1992). <https://doi.org/10.1193/1.1585688>
- [7] Panagiotakos, T.B., Fardis, M.N.: A displacement-based seismic design procedure for RC buildings and comparison with EC8. *Earthq. Eng. Struct. Dyn.* 30, 1439–1462 (2001). <https://doi.org/10.1002/eqe.71>

- [8] Priestley, M.J.N., Kowalsky, M.J.: Direct Displacement-Based Seismic Design of Concrete Buildings. *Bull. New Zeal. Soc. Earthq. Eng.* 33, 421–444 (2000). <https://doi.org/10.5459/bnzsee.33.4.421-444>
- [9] Medhekar, M.S., Kennedy, D.J.L.: Displacement-based seismic design of buildings - application. *Eng. Struct.* 22, 210–221 (2000). [https://doi.org/10.1016/S0141-0296\(98\)00093-5](https://doi.org/10.1016/S0141-0296(98)00093-5)
- [10] Medhekar, M.S., Kennedy, D.J.L.: Displacement-based seismic design of buildings - theory. *Eng. Struct.* 22, 201–209 (2000). [https://doi.org/10.1016/S0141-0296\(98\)00092-3](https://doi.org/10.1016/S0141-0296(98)00092-3)
- [11] Priestley, M.J.N.: Myths and Fallacies in Earthquake Engineering - Conflicts between Design and Reality. *Bull. New Zeal. Soc. Earthq. Eng.* 26, 329–341 (1993)
- [12] Sullivan, T.J., Calvi, G.M., Priestley, M.J.N., Kowalsky, M.J.: The limitations and performances of different displacement based design methods. *J. Earthq. Eng.* 7, 201–241 (2003). <https://doi.org/10.1080/13632460309350478>
- [13] Priestley, M.J.N., Calvi, G.M., Kowalsky, M.J.: *Displacement-Based Seismic Design of Structures*. Pavia, ITALY, IUSS PRESS. ISBN: 978-88-6198-000-6 (2007)
- [14] Sullivan, T.J., Priestley, M.J.N., Calvi, G.M. eds: *A Model Code for the Seismic Design of Structures*. IUSS press Pavia, Italy, Pavia, ITALY (2012)
- [15] Pettinga, J.D., Priestley, M.J.N.: Dynamic behaviour of reinforced concrete frames designed with direct displacement-based design. *J. Earthq. Eng.* 9, 309–330 (2005). <https://doi.org/10.1142/S1363246905002419>
- [16] Sullivan, T.J., Priestley, M.J.N., Calvi, G.M.: Direct displacement-based design of frame-wall structures. *J. Earthq. Eng.* 10, 91–124 (2006). <https://doi.org/10.1080/13632460609350630>
- [17] Moghim, F., Saadatpour, M.M.: The applicability of Direct Displacement-Based Design in designing concrete buildings located in near-fault regions. In: *The 14th World Conference on Earthquake Engineering*. 12-17 October (2008)
- [18] Belleri, A.: *Displacement Based Design for Precast Concrete Structures*. Presented at the (2009)
- [19] Sullivan, T.J., Lago, A.: Towards a simplified Direct DBD procedure for the seismic design of moment resisting frames with viscous dampers. *Eng. Struct.* 35, 140–148 (2012). <https://doi.org/10.1016/j.engstruct.2011.11.010>
- [20] Malekpour, S., Dashti, F.: Application of the Direct Displacement Based Design Methodology for Different Types of RC Structural Systems. *Int. J. Concr. Struct. Mater.* 7, 135–153 (2013). <https://doi.org/10.1007/s40069-013-0043-2>
- [21] Pourali, N., Khosravi, H., Dehestani, M.: An investigation of P-delta effect in conventional seismic design and direct displacement-based design using elasto-plastic SDOF systems. *Bull. Earthq. Eng.* 17, 313–336 (2019). <https://doi.org/10.1007/s10518-018-0460-3>
- [22] Sahoo, D.R., Prakash, A.: Seismic behavior of concentrically braced frames designed using direct displacement-based method. *Int. J. Steel Struct.* 19, 96–109 (2019). <https://doi.org/10.1007/s13296-018-0092-0>

- [23] Yan, L., Gong, J.: Development of displacement profiles for direct displacement based seismic design of regular reinforced concrete frame structures. *Eng. Struct.* 190, 223–237 (2019). <https://doi.org/10.1016/j.engstruct.2019.04.015>
- [24] Giannakouras, P., Zeris, C.: Seismic performance of irregular RC frames designed according to the DDBD approach. *Eng. Struct.* 182, 427–445 (2019). <https://doi.org/10.1016/j.engstruct.2018.12.058>
- [25] Kumbhar, O.G., Kumar, R., Noroozinejad Farsangi, E.: Investigating the efficiency of DDBD approaches for RC buildings. *Structures.* 27, 1501–1520 (2020). <https://doi.org/10.1016/j.istruc.2020.07.015>
- [26] Malla, N., Wijeyewickrema, A.C.: Direct displacement-based design of coupled walls with steel shear link coupling beams. *Structures.* 34, 2746–2764 (2021). <https://doi.org/10.1016/j.istruc.2021.09.004>
- [27] Papagiannopoulos, G.A., Hatzigeorgiou, G.D., Beskos, D.E.: Direct Displacement-Based Design. (2021)
- [28] Sharma, A., Tripathi, R.K., Bhat, G.: Direct-displacement and force-based seismic assessment of RC frame structures. *J. Build. Pathol. Rehabil.* 7, (2022). <https://doi.org/10.1007/s41024-021-00160-z>
- [29] Mohebbi, M., Noruzvand, M., Dadkhah, H., Shakeri, K.: Direct displacement-based design approach for isolated structures equipped with supplemental fluid viscous damper. *J. Build. Eng.* 45, (2022). <https://doi.org/10.1016/j.jobe.2021.103684>
- [30] Kalapodis, N.A., Muho, E. V., Beskos, D.E.: Seismic design of plane steel MRFS, EBFS and BRBFS by improved direct displacement-based design method. *Soil Dyn. Earthq. Eng.* 153, 107111 (2022). <https://doi.org/10.1016/j.soildyn.2021.107111>
- [31] Estekanchi, H.E., Vafai, A., Sadegh, A.M.: Endurance time method for seismic analysis and design of structures. *Sci. Iran.* 11, 361–370 (2004)
- [32] Estekanchi, H.E., Mashayekhi, M., Vafai, H., Ahmadi, G., Mirfarhadi, S.A., Harati, M.: A state-of-knowledge review on the endurance time method. *Structures.* 27, 2288–2299 (2020). <https://doi.org/10.1016/j.istruc.2020.07.062>
- [33] Estekanchi, H.E., Harati, M., Mashayekhi, M.R.: An investigation on the interaction of moment-resisting frames and shear walls in RC dual systems using endurance time method. *Struct. Des. Tall Spec. Build.* 27, 1–16 (2018). <https://doi.org/10.1002/tal.1489>
- [34] Mashayekhi, M., Harati, M., Estekanchi, H.E.: Development of an alternative PSO-based algorithm for simulation of endurance time excitation functions. *Eng. Reports.* 1, 1–15 (2019). <https://doi.org/10.1002/eng2.12048>
- [35] Mashayekhi, M., Estekanchi, H.E., Vafai, H.: Simulation of Endurance Time Excitations via Wavelet Transform. *Iran. J. Sci. Technol. - Trans. Civ. Eng.* 43, 429–443 (2019). <https://doi.org/10.1007/s40996-018-0208-y>
- [36] Shirkhani, A., Farahmand Azar, B., Charkhtab Basim, M.: Optimum slip load of T-shaped friction dampers in steel frames by endurance time method. *Proc. Inst. Civ. Eng. Struct. Build.* 173, 746–760 (2020). <https://doi.org/10.1680/jstbu.18.00169>

- [37] Shirkhani, A., Farahmand Azar, B., Charkhtab Basim, M.: Evaluation of efficiency index of friction energy dissipation devices using endurance time method. *Numer. Methods Civ. Eng.* 5, 12–20 (2020). <https://doi.org/10.52547/nmce.5.2.12>
- [38] Hariri-Ardebili, M.A., Sattar, S., Estekanchi, H.E.: Performance-based seismic assessment of steel frames using endurance time analysis. *Eng. Struct.* 69, 216–234 (2014). <https://doi.org/10.1016/j.engstruct.2014.03.019>
- [39] Amouzegar, H., Riahi, H.T.: Seismic assessment of concrete frames by endurance time method. *Proc. Inst. Civ. Eng. Struct. Build.* 168, 578–592 (2015). <https://doi.org/10.1680/stbu1400042>
- [40] Mashayekhi, M., Estekanchi, H.E., Vafai, A., Mirfarhadi, S.A.: Simulation of Cumulative Absolute Velocity Consistent Endurance Time Excitations. *J. Earthq. Eng.* 25, 892–917 (2018). <https://doi.org/10.1080/13632469.2018.1540371>
- [41] Shirkhani, A., Mualla, I.H., Shabakhty, N., Mousavi, S.R.: Behavior of steel frames with rotational friction dampers by endurance time method. *J. Constr. Steel Res.* 107, 211–222 (2015). <https://doi.org/10.1016/j.jcsr.2015.01.016>
- [42] Mashayekhi, M., Estekanchi, H.E., Vafai, H., Mirfarhadi, S.A.: Development of hysteretic energy compatible endurance time excitations and its application. *Eng. Struct.* 177, 753–769 (2018). <https://doi.org/10.1016/j.engstruct.2018.09.089>
- [43] Basim, M.C., Estekanchi, H.E.: Application of endurance time method in performance-based optimum design of structures. *Struct. Saf.* 56, 52–67 (2015). <https://doi.org/10.1016/j.strusafe.2015.05.005>
- [44] Riahi, H.T., Estekanchi, H.E.: Seismic assessment of steel frames with the endurance time method. *J. Constr. Steel Res.* 66, 780–792 (2010). <https://doi.org/10.1016/j.jcsr.2009.12.001>
- [45] Shirkhani, A., Farahmand Azar, B., Charkhtab Basim, M.: Seismic loss assessment of steel structures equipped with rotational friction dampers subjected to intensifying dynamic excitations. *Eng. Struct.* 238, 112233 (2021). <https://doi.org/10.1016/j.engstruct.2021.112233>
- [46] TSC: Turkish Seismic Design Code : Specification for Structures to be Built in Disaster Areas. Ministry of Public Works and Settlement Government of Republic of Turkiye (2007)
- [47] TBEC: Turkish Building Earthquake Code. The Disaster and Emergency Management Authority (AFAD), Ankara , Turkiye. (2018)
- [48] TS-500: Requirements for Design and Construction of Reinforced Concrete Structures. English version, publication NO.2003/1. Turkish Standards Institute, Ankara Turkiye. (2000)
- [49] Ersoy, U., Özcebe, G., Tankut, T.: Reinforce Concrete. METU Press. ISBN:978-605-4362-17-2, Middle East Technical University (METU), Ankara, Turkiye (2013)
- [50] Soyuluk, A., Harmankaya, Z.Y.: The History of Development in Turkish Seismic Design Codes. *Int. J. Civ. Environ. Eng.* 12, 25–29 (2012)
- [51] Atmaca, N., Atmaca, A., Kılçık, S.: Comparison of 2018 and 2007 Turkish Earthquake Regulations. *Int. J. Energy Eng. Sci.* 4, 19–25 (2019)

- [52] Aksoylu, C., Mobark, A., Arslan, M.H., Erkan, I.H.: A comparative study on ASCE 7-16, TBEC-2018 and TEC-2007 for reinforced concrete buildings. *Rev. la Constr.* 19, 282–305 (2020). <https://doi.org/10.7764/RDLC.19.2.282>
- [53] Džaki, D., Kraus, I., Mori, D.: Direct Displacement Based Design of Regular Concrete Frames in Compliance With Eurocode 8. 19, 973–982 (2012)
- [54] Pettinga, J.D.: *Dynamic Behaviour of Reinforced Concrete Frames Designed with Direct Displacement-Based Design*, (2005)
- [55] Massena, B., Bento, R., Degée, H.: Direct displacement based design of a RC frame – Case of study. (2010)
- [56] Priestley, M.J.N., Calvi, G.M., Kowalsky, M.J.: Direct Displacement-Based Seismic Design of Structures. In: NZSEE Conference. , New Zealand, 2007 (2007)
- [57] Habibi, A., Gholami, R., Izadpanah, M.: Behavior factor of vertically irregular RCMRFs based on incremental dynamic analysis. *Earthq. Struct.* 16, 655–664 (2019). <https://doi.org/10.12989/eas.2019.16.6.655>
- [58] Fayed, M.N., Nasr, N.E., Saleh, M., Ahmed, G.M.: Seismic Response Modification factors for Multi-Story R.C buildings having Flat Slab System. *IOSR J. Mech. Civ. Eng.* 17, 1–14 (2020). <https://doi.org/10.9790/1684-1701050114>
- [59] Hussein, M.M., Gamal, M., Attia, W.A.: Seismic response modification factor for RC-frames with non-uniform dimensions. *Cogent Eng.* 8, (2021). <https://doi.org/10.1080/23311916.2021.1923363>
- [60] Mahmoudi, M., Zaree, M.: Evaluating response modification factors of concentrically braced steel frames. *J. Constr. Steel Res.* 66, 1196–1204 (2010). <https://doi.org/10.1016/j.jcsr.2010.04.004>
- [61] Mohamed, A.E., Attia, W.A., El-Degwy, W.M.: Seismic Response Modification Factor of Reinforced Concrete Frames Based on Pushover Analysis. *J. Archit. Environ. Struct. Eng. Res.* 2, 2–10 (2019). <https://doi.org/10.30564/jaeser.v2i2.818>
- [62] Mwafy, A.M., Elnashai, A.S.: Calibration of force reduction factors of RC buildings. *J. Earthq. Eng.* 6, 239–273 (2002). <https://doi.org/10.1080/13632460209350416>
- [63] Zahrai, S.M., Khorraminejad, A., Sedaghati, P.: Response modification factors of concrete bridges with different bearing conditions. *Earthq. Struct.* 16, 185–196 (2019). <https://doi.org/10.12989/eas.2019.16.2.185>
- [64] Pérez, J.C.V., Loachamín, M.A.C.: Calibration of the response reduction factors used in Ecuador for steel SMRF. *Bull. Int. Inst. Seismol. Earthq. Eng.* 52, 22–37 (2018)
- [65] Sadeghi, A., Abdollahzadeh, G., Rajabnejad, H., Naseri, S.A.: Numerical analysis method for evaluating response modification factor for steel structures equipped with friction dampers. *Asian J. Civ. Eng.* 22, 313–330 (2021). <https://doi.org/10.1007/s42107-020-00315-2>
- [66] Miranda, E., Bertero, V. V.: Evaluation of Strength Reduction Factors for Earthquake-Resistant Design. *Earthq. Spectra.* 10, 357–379 (1994). <https://doi.org/10.1193/1.1585778>
- [67] ATC-19: Structural Response Modification Factors. Applied Technology Council, 555 Twin Dolphin Drive, Suite 550, Redwood City, California. (1995)

- [68] Estekanchi, H.E., Vafai, A., Riahi, H.T.: Endurance Time Method: From ideation to Application. In: US-Iran Seismic Workshop. bl 205–218 (2009)
- [69] Vamvatsikos, D., Allin Cornell, C.: Incremental dynamic analysis. *Earthq. Eng. Struct. Dyn.* 31, 491–514 (2002). <https://doi.org/10.1002/eqe.141>
- [70] Azarbakht, A., Dolsek, M.: Prediction of the median IDA curve by employing a limited number of ground motion records. *Earthq. Eng. Struct. Dyn.* 36, 2401–2421 (2007). <https://doi.org/DOI: 10.1002/eqe.740> Prediction
- [71] Mashayekhi, M., Harati, M., Ashoori Barmchi, M., Estekanchi, H.E.: Introducing a response-based duration metric and its correlation with structural damages. *Bull. Earthq. Eng.* 17, 5987–6008 (2019). <https://doi.org/10.1007/s10518-019-00716-y>
- [72] Hancock, J., Bommer, J.J.: Using spectral matched records to explore the influence of strong-motion duration on inelastic structural response. *Soil Dyn. Earthq. Eng.* 27, 291–299 (2007). <https://doi.org/10.1016/j.soildyn.2006.09.004>
- [73] Harati, M., Mashayekhi, M., Ashoori Barmchi, M., Estekanchi, H.: Influence of Ground Motion Duration on the Structural Response at Multiple Seismic Intensity Levels. *Numer. Methods Civ. Eng.* 3, 10–23 (2019). <https://doi.org/10.29252/nmce.3.4.10>
- [74] Mashayekhi, M., Harati, M., Darzi, A., Estekanchi, H.E.: Incorporation of strong motion duration in incremental-based seismic assessments. *Eng. Struct.* 223, 111144 (2020). <https://doi.org/10.1016/j.engstruct.2020.111144>
- [75] Cabanas, L., Benito, B., Herraiz, M.: An Approach To the Measurement of the Potential Structural Damage of Earthquake Ground Motions. *Earthq. Eng. Struct. Dyn.* 26, 79–92 (1997). [https://doi.org/10.1002/\(SICI\)1096-9845\(199701\)26:1<79::AID-EQE624>3.0.CO;2-Y](https://doi.org/10.1002/(SICI)1096-9845(199701)26:1<79::AID-EQE624>3.0.CO;2-Y)
- [76] Reed, J.W., Kassawara, R.P.: A criterion for determining exceedance of the operating basis earthquake. *Nucl. Eng. Des.* 123, 387–396 (1990). [https://doi.org/10.1016/0029-5493\(90\)90259-Z](https://doi.org/10.1016/0029-5493(90)90259-Z)
- [77] Campbell, K.W., Bozorgnia, Y.: A comparison of ground motion prediction equations for arias intensity and cumulative absolute velocity developed using a consistent database and functional form. *Earthq. Spectra.* 28, 931–941 (2012). <https://doi.org/10.1193/1.4000067>
- [78] Harati, M., Mashayekhi, M., Estekanchi, H.E.: Correlation of ground motion duration with its intensity metrics: A simulation based approach. *J. Soft Comput. Civ. Eng.* 4, 17–39 (2020). <https://doi.org/10.22115/SCCE.2020.227576.1207>
- [79] FEMA-P695: Quantification of building seismic performance factors. Federal Emergency Management Agency, Washington, DC (2009)
- [80] Estekanchi, H.E., Valamanesh, V., Vafai, A.: Application of Endurance Time method in linear seismic analysis. *Eng. Struct.* 29, 2551–2562 (2007). <https://doi.org/10.1016/j.engstruct.2007.01.009>

Appendix

The reinforcement details are provided in the following figures for the elements of all structures.

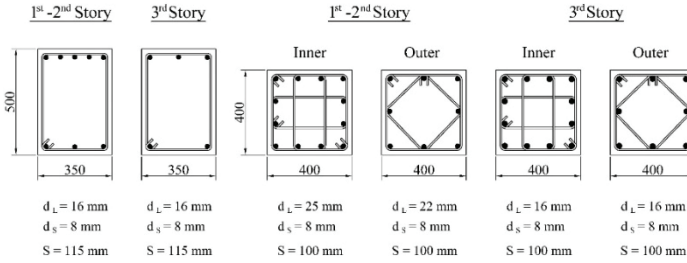


Figure A.1 - Cross-sections of columns and beams for 3-Story structure designed using the DDBD approach in accordance with TSC-2007.

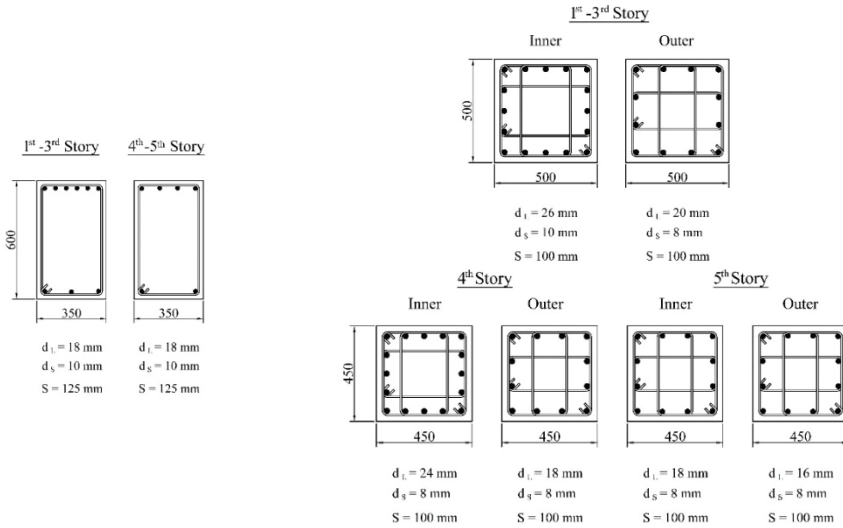


Figure A.2 - Cross-sections of columns and beams for 5-Story structure designed using the DDBD approach in accordance with TSC-2007.

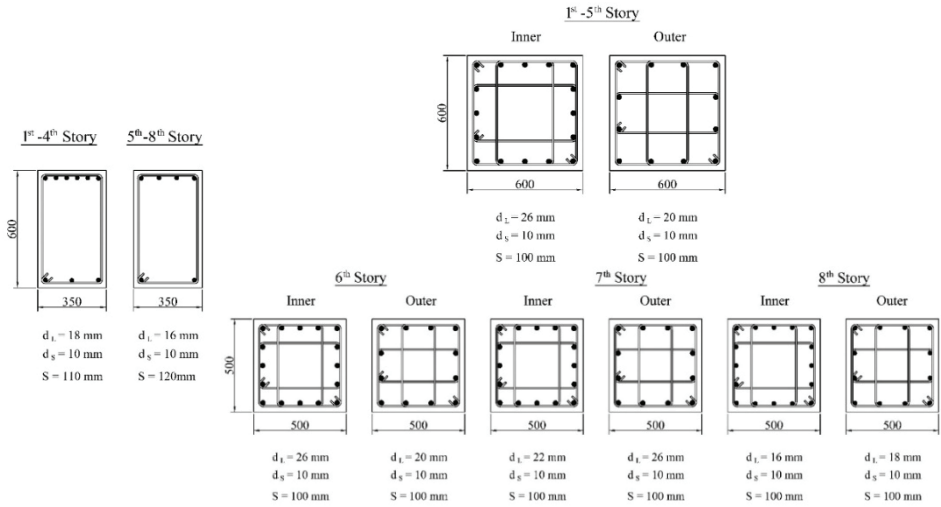


Figure A.3 - Cross-sections of columns and beams for 8-Story structure designed using the DDBD approach in accordance with TSC-2007.

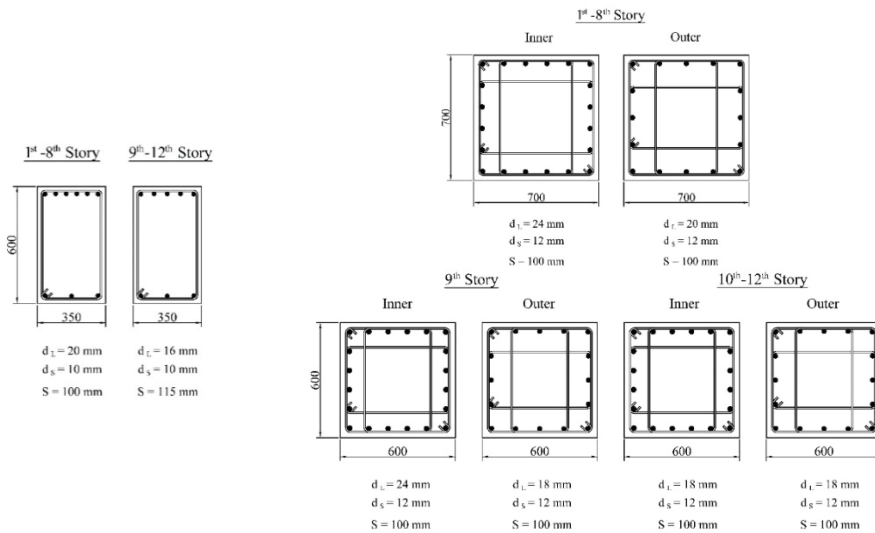


Figure A.4 - Cross-sections of columns and beams for 12-Story structure designed using the DDBD approach in accordance with TSC-2007.

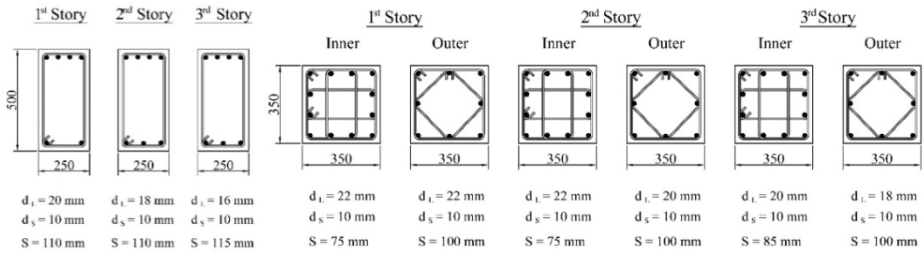


Figure A.5 - Cross-sections of columns and beams for 3-Story structure designed using the DDBD approach in accordance with TBEC-2018.

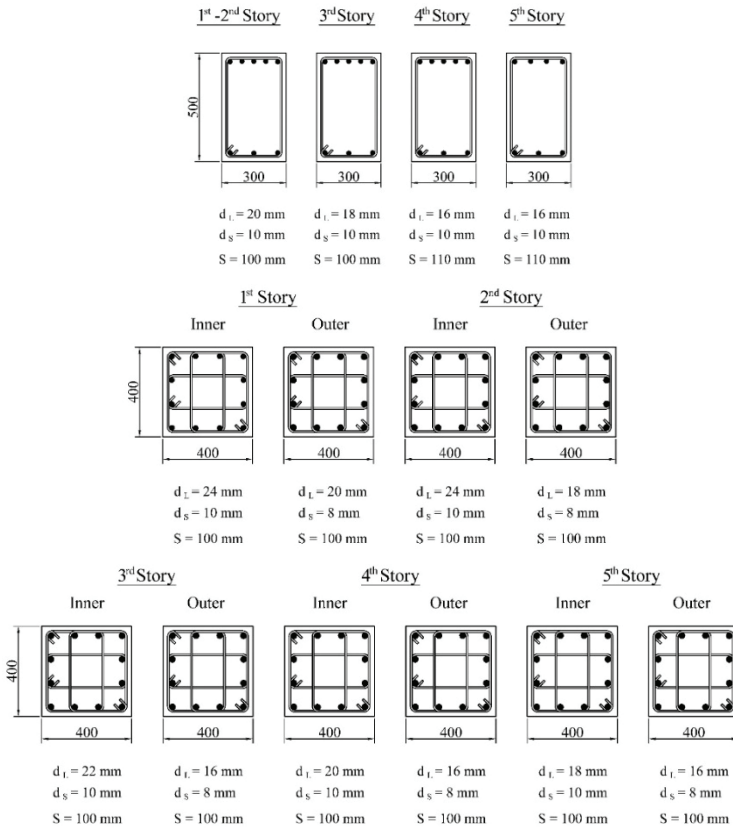


Figure A.6 - Cross-sections of columns and beams for 3-Story structure designed using the DDBD approach in accordance with TBEC-2018.

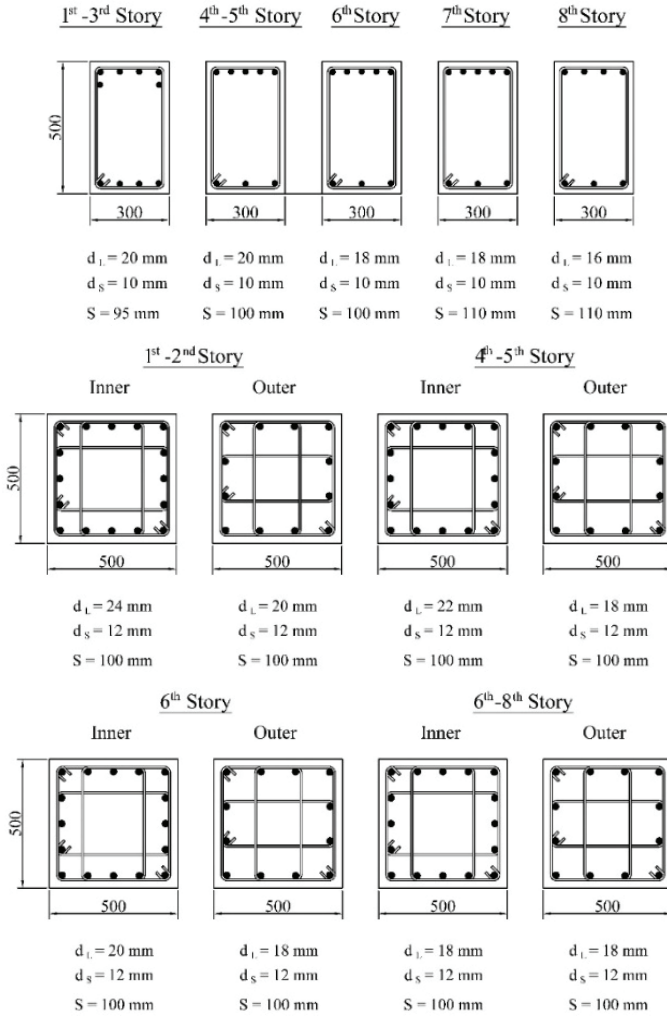


Figure A.7 - Cross-sections of columns and beams for 8-Story structure designed using the DDBD approach in accordance with TBEC-2018.

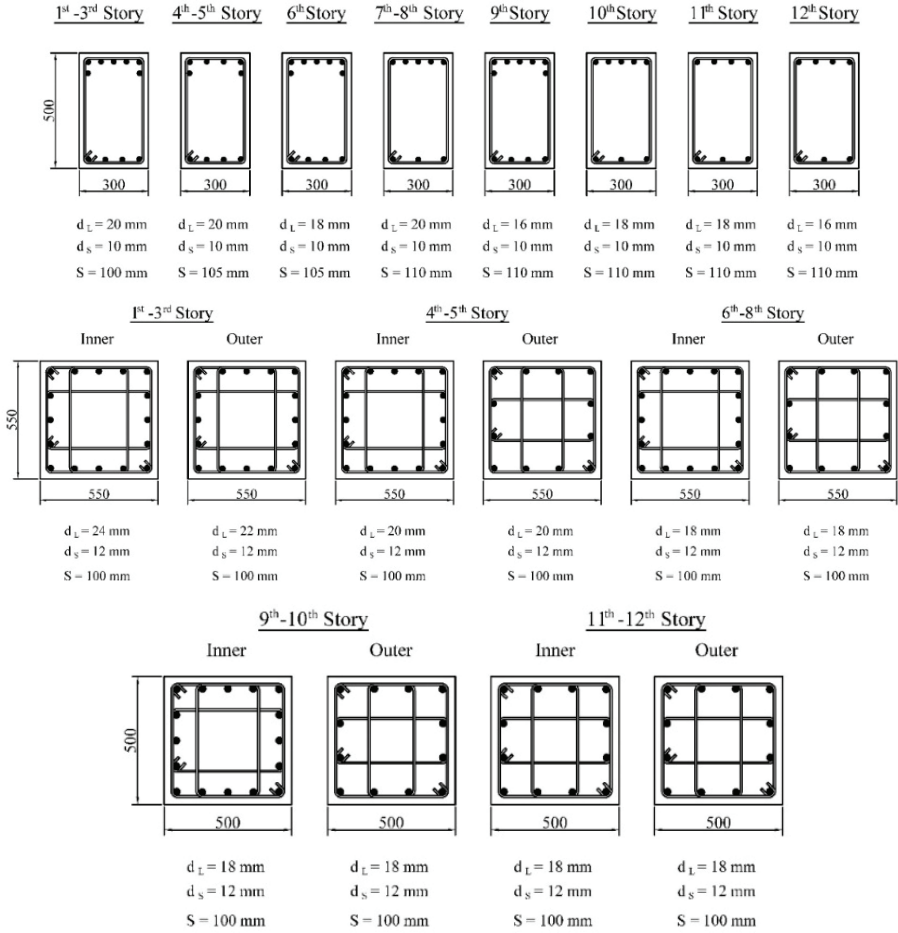


Figure A.8 - Cross-sections of columns and beams for 12-Story structure designed using the DDBD approach in accordance with TBEC-2018.